Assessing the Source of the Photochemical Formation of Hydroxylating Species from Dissolved Organic Matter Using Model Sensitizers

by

Kylie Dawn Couch

B.S., California State University Long Beach, 2016

A thesis submitted to the

Faculty of the Graduate School of the

University of Colorado in partial fulfillment

of the requirement for the degree of

Master of Science

Environmental Engineering Program

2021

Committee Members:

Fernando L. Rosario-Ortiz

Cresten Mansfeldt

Garrett McKay

Couch, Kylie Dawn (M.S., Environmental Engineering Program)

Assessing the Source of the Photochemical Formation of Hydroxylating Species from Dissolved Organic Matter Using Model Sensitizers

Thesis directed by Professor Fernando L. Rosario-Ortiz

Dissolved organic matter (DOM) is ubiquitous in natural waters and can facilitate the chemical transformation of many contaminants through the photochemical production of reactive intermediates, such as singlet oxygen ($^1O_2$), excited triplet state DOM (^{3}DOM*), and hydroxylating species ($^{\bullet}$OH and other intermediates of similar reaction chemistry). The formation mechanism of most reactive intermediates is well understood, but this is not the case for the formation of hydroxylating species from DOM. To investigate this chemistry DOM model sensitizers were irradiated with two different probe compounds (benzene and benzoic acid) at two irradiation wavelengths (254 and 320 nm). The ability of DOM model sensitizers to hydroxylate these arene probes was assessed by measuring rates of formation of the hydroxylated probe compounds (phenol and salicylic acid). Multiple classes of model sensitizers were tested, including quinones, hydroxybenzoic acids, aromatic ketones, and other triplet forming species. Of these classes of model sensitizers, only quinones and hydroxybenzoic acids had a hydroxylating capacity. Methanol quenching experiments were used to assess the reactivity of hydroxylating species. These results have several implications for the systems tested. First, they show that methanol is not useful in differentiating $^{\bullet}$OH from $^{\bullet}$OH-like species. Also, they suggest that the hydroxylating intermediate produced from hydroxybenzoic acid photolysis may not be hydroxyl radical, but a different hydroxylating species. Lastly, these data prompted investigation of whether quinone photoproducts have a hydroxylating capacity. To evaluate this photochemistry experiments were performed with a p-benzoquinone

photoproduct, hydroquinone. This data shows that hydroquinone has a hydroxylating capacity and that this likely contributes to the quinone-related production of hydroxylating species from DOM photolysis. These results confirm that hydroxybenzoic acids and quinones are important to the photochemical production of hydroxylating species from DOM, but the mechanism by which this occurs for these classes of sensitizers is still elusive. Ultimately, these findings contribute to the growing understanding of the role individual molecular moieties play in DOM photochemistry.

Dedication

I dedicate this thesis to the part of myself that I am letting go of as I finish this degree. The person who thought the only path to worthiness was perfection and who taught me what it means to be flawed, and therefore human.

Acknowledgements

I would like to thank my advisor, Dr. Fernando Rosario-Ortiz, for his help and advice with this project. Thank you to the National Science Foundation for funding this project.

I would also like to thank Dr. Garrett McKay, who mentored me in the early days of graduate school. You are an incredible researcher and friend.

Dr. Cresten Mansfeldt, I am deeply grateful to have met you during this process. You are a truly inspiring mentor. Thank you for your support through hard times.

Dr. Frank Leresche, thank you for your willingness to share your immense knowledge with me. This thesis would not be what it is without you.

I am grateful for the connections I made with other researchers through this process, including Dr. Sarah Fischer, Dr. Sydney Ulliman, Ariel Retuta, Claire Farmer, and all of the members of the Rosario lab group. Thank you for your support and the countless conversations that helped guide me through difficult moments. I cannot begin to express my gratitude for the support I have gotten from my colleague and friend, Kaitlyn Jeanis. Thank you for the countless hours you spent listening to me practice presentations and proofreading my writing.

Finally, I would like to thank my parents, who have unwaveringly supported me throughout my life.

Contents

List of Tables

List of Figures

List of Equations

List of Abbreviations

3MP – 3-methoxyacetophenone

4BA – 4-benzoylbenzoic acid

4HBA – 4-hydroxybenzoic acid

A2S – anthraquinone-2-sulfonic acid

$A2S^{\bullet-}$ – semiquinone radical for parent compound anthraquinone-2-sulfonate

BA – Benzoic acid

DHBA – 2,4-dihydroxybenzoic acid

DOM – Dissolved organic matter

^{3}DOM* – Triplet state DOM

DMPO – 5,5-dimethyl-1-pyrroline-1-oxide

DMSO – dimethyl sulfoxide

DPBQ – 2,6-dimethoxy-*p*-benzoquinone

EAC – Electron accepting capacity

EDC – Electron donating capacity

EPR – Electron paramagnetic resonance spectroscopy

$E^0_{\mathrm{p,total}}$ – total photon irradiance of Rayonet reactor

$\varepsilon_{\lambda,PC}$ – Molar extinction coefficient of probe compound

$\varepsilon_{\lambda,Sens}$ – Molar extinction coefficient of Sens

$\varepsilon_{\mathrm{uridine}}$ – Molar extinction coefficient for uridine at 254 nm

FT-ICR MS – Fourier transform ion cyclotron resonance mass spectrometry

f – fraction of $^{\bullet}$OH reacting with the probe compounds in the presence of other species

f_{Sens} – fraction of light absorbed by Sens in experimental solutions

H_2O_2 – Hydrogen peroxide

[H_2O_2] – concentration of hydrogen peroxide

HPLC – High performance liquid chromatography

$k_{\mathrm{BA,3PBQ*}}$ – second order rate constant for reaction of triplet PBQ with BA

$k_{\mathrm{H2O,3PBQ*}}$ – second order rate constant for reaction of triplet PBQ with water

$k_{\mathrm{MeOH,\bullet OH}}$ – second order rate constant for reaction of •OH with MeOH

$k_{\mathrm{MeOH,3PBQ*}}$ – second order rate constant for reaction of triplet PBQ with MeOH

$k_{\mathrm{O2,3PBQ*}}$ – second order rate constant for reaction of triplet PBQ with O_2

$k_{\mathrm{PC,\bullet OH}}$ – second order rate constant for reaction of •OH with probe compound

$k_{\mathrm{Sens,\bullet OH}}$ – second order rate constant for reaction of •OH with Sens

$k_{\mathrm{Sens}-a}$ – specific rate of light absorption by Sens

l – Optical pathlength

MeOH – Methanol

[MeOH] – concentration of methanol

•OH – Hydroxyl radical

$^1O_2$ – Singlet oxygen

PBQ – *p*-benzoquinone

PC – Probe compound

[PC] – Concentration of probe compoun

PNA – *p*-Nitroanisole

PYR – pyridine

[PYR] – concentration of pyridine

ρ_λ – relative spectral photon irradiance

$\Phi_{\bullet OH}$ – Quantum yield for the production of hydroxylating species

Φ_{PNA} – Quantum yield for PNA/PYR actinometer

$\Phi_{uridine}$ – Quantum yield for uridine actinometer

$R_{\bullet OH}$ – Rate of formation of hydroxylating species

R_{PC-OH} – rate of formation of the hydroxylated probe compound

RI – Reactive intermediates

Sens – Model sensitizer

[Sens] – Concentration of Sens

SRFA – Suwannee River fulvic acid

$S_{\lambda,PC,Sens}$ – Light screening factor

TCA – *trans*-cinnamic acid

UMI – umbelliferone

$[uridine]_0$ – initial concentration of uridine

$Y_{\bullet OH}$ – yield of reaction of •OH with the probe compound

$Y_{\bullet OH-like}$ – yield of reaction of •OH-like species with probe compound

INTRODUCTION

Dissolved organic matter (DOM) is the primary light absorbing species in natural waters and has been shown to facilitate the chemical transformation of various contaminants through the production of reactive intermediates (RI).[1–5] These RI, which include singlet oxygen ($^1O_2$), excited triplet state DOM (^{3}DOM*), and hydroxylating species ($^{\bullet}$OH and other intermediates of similar reaction chemistry), can react with many contaminants, making them important participants in the photodegradation of contaminants in natural waters and in engineered systems.[6–12]

The formation mechanisms for most RI are well understood;[10,13,14] however, this is not the case for the formation of hydroxylating species from DOM. DOM photohydroxylation mechanisms can be differentiated experimentally by the involvement (or lack thereof) of hydrogen peroxide (H_2O_2) and/or dissolved oxygen.[2] The H_2O_2-dependent pathway involves Fenton-like reactions [1,15,16] and results in the direct formation of $^{\bullet}$OH, whereas the H_2O_2-independent pathway involves the production of hydroxylating species directly through photochemical reactions involving DOM. The precise mechanism by which hydroxylating species are produced from DOM photolysis (H_2O_2-independent pathway) has remained elusive, in terms of both the chemical moieties involved and identity of the oxidant. Although early studies attributed DOM photohydroxylation reactions to $^{\bullet}$OH [2,17], a study by Page et al. (2011)[18] suggests that the production of hydroxylating species from DOM photolysis may not exclusively be $^{\bullet}$OH, prompting the acknowledgement of yet-unknown hydroxylating species that is also formed through photochemical reactions of DOM. These so-called $^{\bullet}$OH-like species have been invoked,[19–21] which have lower, but not well-defined, reactivity compared to $^{\bullet}$OH.[21] A primary difficulty in teasing apart the role of $^{\bullet}$OH versus so-called $^{\bullet}$OH-like species is that photohydroxylation reactions with many organic molecules result in identical products.[13]

The identity of OH-like species is somewhat ambiguous, but the current understanding is that these species are either excited states or excited state complexes of chromophores within DOM. Previous studies have employed model sensitizers (Sens) to assess potential mechanisms for the H_2O_2-independent pathway by which OH-like species are produced.[10,19,21–25] These sensitizers are selected based on their presence in DOM (e.g. quinones, aromatic ketones, aromatic acids) and whether they are photochemically active. Even if these groups are part of larger molecular weight structures, it is believed that the use of the model sensitizers is still warranted as it could be expected that these functionalities will still represent the primary photochemically active part of DOM. Notably, DOM absorbance can be interpreted using a superposition model or a charge-transfer model. The use of individual model sensitizers invokes the superposition model, which is justified in this study because the irradiation wavelengths chosen (254 and 320 nm) excite local states, not charge transfer states, which are hypothesized to occur mainly at 350 nm excitation or longer. Also, recent studies[26,27] have shown that charge-transfer transitions may not be as prevalent as originally hypothesized.[28,29]

Similar to other RI, •OH and other hydroxylating species can be quantified using probe compounds.[13,30] Some probe compounds that have been used for the detection of hydroxylating species from DOM photolysis are dimethyl sulfoxide, methane, benzene, nitrobenzene, benzoic acid, *p*-chlorobenzoic acid, and terephthalic acid.[13,19,23,31–33] These probe compounds react either by hydrogen atom abstraction (e.g., methane) or hydroxylation (e.g. DMSO, arenes).[13] Ideally, probe compounds would be selective for reaction with •OH or •OH-like species, but there is evidence that •OH-like species react with some probe compounds in a way that is indistinguishable from •OH reaction.[18,20,21] Due to their lack of selectivity, most probe compounds measure the hydroxylating capacity of a given system, which encompasses the measurement of both •OH and

other hydroxylating species. Methane is the only probe thought to be selective for •OH, due to its high H-C bond dissociation energy. For this reason, methane has been used to distinguish between •OH and •OH-like species.[18,19]

Some Sens that have been shown to produce hydroxylating species upon irradiation include quinones and hydroxybenzoic acids.[19,21,22,32,34–36] Early studies of the photochemical production of a hydroxylating intermediate from quinone photochemistry utilized a spin trap probe, 5,5-dimethyl-1-pyrroline-1-oxide (DMPO).[32,34–36] These studies claimed that the •OH is formed via H-atom abstraction when triplet quinones react with water. However, a number of studies have shown that there are other photochemical pathways that occur in the presence of triplet quinones that yield the same product as the reaction between DMPO and •OH.[37–39] For this reason, conclusions from earlier studies that utilized DMPO as probe compound are not reliable. Other studies have been performed using dimethyl sulfoxide (DMSO) as a probe compound to assess the chemical behavior of the hydroxylating intermediate produced from 2-methyl-*p*-benzoquinone photolysis by measuring the production of methyl radicals from the reaction of the hydroxylating intermediate with DMSO.[19,21] However, a few studies have presented data that brings the use of DMSO as a probe for hydroxylating species into question.[37,40] Von Sonntag et al. (2004) tested DMSO as a probe for hydroxylating species produced from *p*-benzoquinone photolysis and did not detect methyl radicals, suggesting that there is no oxidizing intermediate and that *p*-benzoquinone undergoes direct photodegradation for form its photoproducts.[37] Interestingly, Gorner (2006) utilized DMSO as a probe and did observe the production of methyl radical, but attributed it to the reaction of the triplet quinone with DMSO.[40] This contradictory data makes DMSO a questionable probe compound and is the reason DMSO was not used in this study. Additionally, Gan et al. (2008) used methane as a probe and established that the hydroxylating intermediate produced from 2-methyl-*p*-

benzoquinone photolysis is not •OH.[19] The same study hypothesizes that the unknown hydroxylating intermediate is a quinone–water exciplex. Overall, the identity of the hydroxylating species produced from quinone photolysis and the mechanism by which this happens are still in question. Considering hydroxybenzoic acids, one previous study that utilized benzene and methane as a probe compounds concluded that this class of sensitizers produce •OH when photolyzed at wavelengths between 290 and 330 nm.[22] This study suggested that, among other possible mechanisms, photooxidation followed by water addition and subsequent •OH cleavage may produce •OH.[22]

The production of hydroxylating species from the photolysis of DOM in surface waters and engineered systems is important because these chemical species can facilitate the transformation of contaminants. Assessing the reactivity of •OH-like species and how it differs from that of •OH is key for understanding and predicting the degradation pathways of chemical contaminants in water. This study focused on three objectives. First, the production of hydroxylating species during photolysis of various classes of model sensitizers was investigated. Second, the possibility that different chemical mechanisms were responsible for this hydroxylating capacity was assessed by utilizing different arene probe compounds and methanol as a quencher. Third, apparent quantum yields of hydroxylated probe compound formation from the Sens in this study were compared to apparent •OH quantum yields from DOM photolysis. Overall, this work contributes to a larger understanding of the photochemistry of DOM in natural waters and engineered systems as it applies to the fate and transport of contaminants.

MATERIALS AND METHODS

Selection of Model Sensitizers

Sens were selected to include chemical species that have been shown to produce hydroxylating species upon photolysis, such as quinones [19,21,41,42] and hydroxybenzoic acids.[22] Additional compounds were selected that exhibit triplet state photochemistry but have not been shown to produce hydroxylating species as a negative control. Model sensitizers selected include *p*-benzoquinone (PBQ), anthraquinone-2-sulfonic acid (A2S), 2,6-dimethoxy-*p*-benzoquinone (DPBQ), 4-hydroxybenzoic acid (4HBA), 2,4-dihydroxybenzoic acid (DHBA), umbelliferone (UMI), *trans*-cinnamic acid (TCA), 4-benzoylbenzoic acid (4BA), and 3-methoxyacetophenone (3MP). These included aromatic ketones and other excited triplet forming species. All Sens structures are presented in Figure 1 with their corresponding triplet state energy and triplet state one electron reduction potentials. Although A2S is likely not the best model for quinone structures in DOM, it was selected because previous studies have used this compound to explore quinone photochemistry and model DOM photochemistry.[23,34,43]

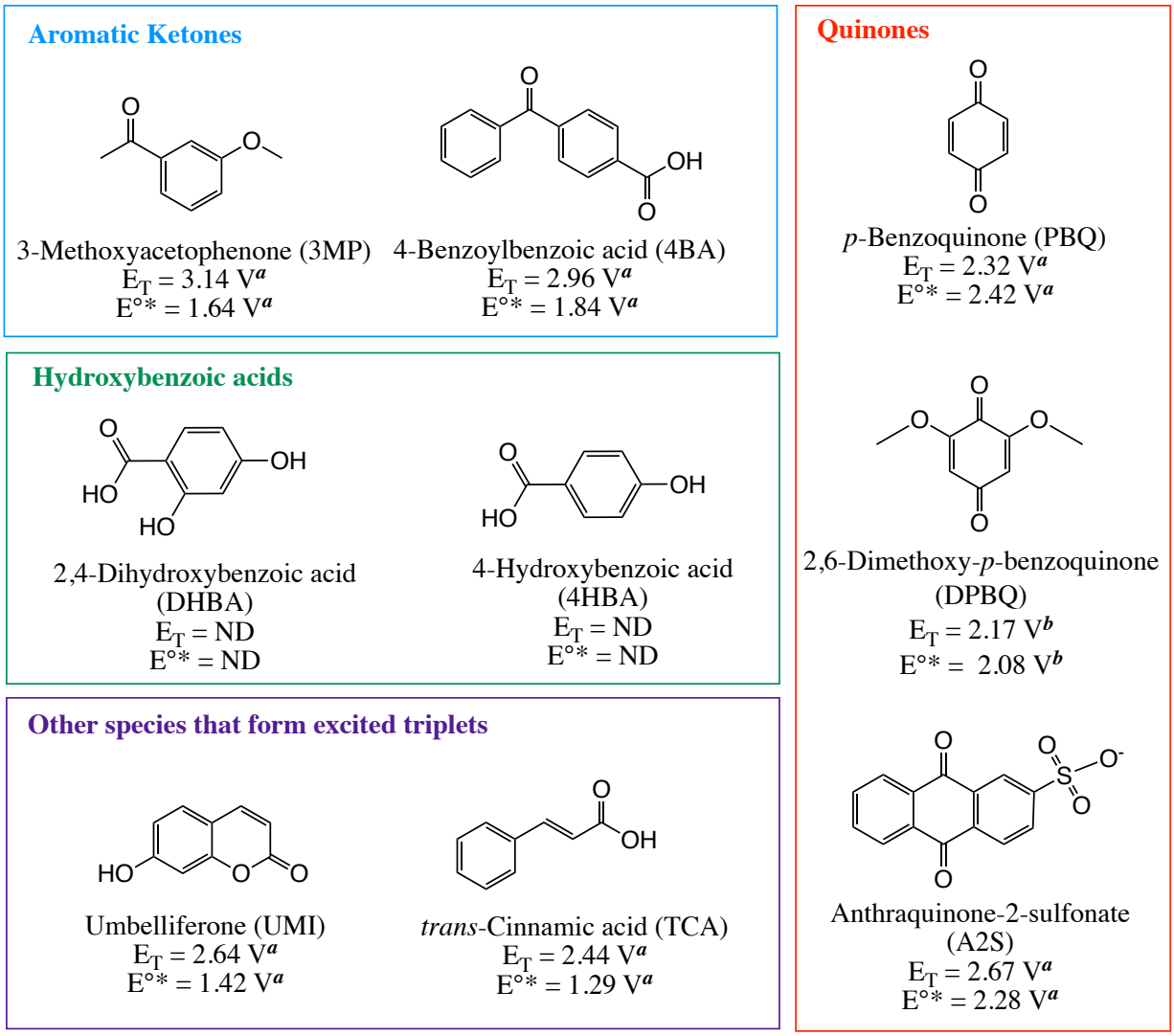

Figure 1. Model sensitizers used in this study, their structures, triplet state one electron reduction potentials (E°*), and triplet energies (E_T). ND = No Data, [a]McNeill and Canonica (2016), [b]Vaughan et al. (2010)

Chemicals and solutions

All chemicals were purchased from commercial sources and are listed in the Table 1 with their respective CAS numbers and purities. Nitrate and nitrite were used as sources of •OH. Solutions were prepared in MilliQ water, with the pH adjusted to 7.0 ± 0.1 using sodium hydroxide (~ 20 mM). Samples were not prepared in buffers to avoid complicating the chemistry of the hydroxylating intermediates, which has been observed in systems containing *p*-benzoquinone in which

the triplet *p*-benzoquinone reacts with phosphate to form an intermediate, *p*-benzoquinone-2-phosphate.[37] During experiments performed with unbuffered solutions there was approximately 0.5 unit decrease in pH from the original pH of 7.0 ± 0.1. All model sensitizers besides UMI (pKa ~7.8) would be unaffected by this pH change. In the case of UMI, a decrease in 0.5 pH units would change the fraction of deprotonated species from 0.13 to 0.044. The photochemistry being observed for UMI is primarily that of the protonated species.

Table 1. List of chemicals, vendors, and chemical purities.

Chemical	***CAS***	***Source***	***Purity***
Benzene	71-43-2	Alfa Aesar	99.8
Phenol	108-95-2	Alfa Aesar	≥99
Benzoic acid	65-85-0	Alfa Aesar	Recrystallized
Salicylic acid	69-72-7	EMD	≥99
p-Benzoquinone	106-51-4	Alfa Aesar	Sublimated
Anthraquinone-2-sulfonate	131-08-8	Aldrich	97%
2,6-Dimethoxy-p-benzoquinone	530-55-2	Alfa Aesar	98%
4-Benzoylbenzoic acid	611-95-0	Aldrich	99%
3-Methoxyacetophenone	586-37-8	Acros Organics	98%
Umbelliferone	93-35-6	Aldrich	99%
trans-Cinnamic acid	140-10-3	Aldrich	≥99%
2,4-Dihydroxybenzoic acid	89-86-1	Aldrich	97%
4-Hydroxybenzoic acid	99-96-7	Aldrich	≥99%
Sodium Nitrate	7631-99-4	Fisher Scientific	99.7%
Sodium Nitrite	7632-00-0	Aldrich	≥97%
Hydrogen peroxide	7722-84-1	BDH	30% w/w
Methanol	67-56-1	VWR	99.8%
Acetonitrile	75-05-8	VWR	99.95%
Phosphoric acid	7664-38-2	EMD	85% w/w
Sodium hydroxide	1310-73-2	Sigma Aldrich	≥97%

Quantification of hydroxylating species

Many probe compounds are available for detection of hydroxylating species, but probes relying on aromatic ring hydroxylation are certainly the most widely used in the aquatic photochemistry community.[20,22,23,31] This was the main motivation for the choice of probes in this study, which were benzene and benzoic acid. Exploration of the chemistry of hydroxylating species with

these two commonly used aromatic probes is important because of the frequency with which they are used to study the production of hydroxylating species from DOM. These results are important to previous studies that employ benzene or benzoic acid as probes for the production of hydroxylating species from DOM photolysis.

The formation of hydroxylating species was detected by monitoring the hydroxylated product of the reaction between the probe compound and hydroxylating species. In the cases of benzoic acid and benzene, the formation of salicylic acid and phenol were monitored, respectively. Rate constants for quenching of •OH with benzene and benzoate are 7.8×10^9 and 5.9×10^9 M^{-1} s^{-1}, respectively.[7]

Analytical instrumentation

Analysis of salicylic acid and phenol was performed with an Agilent 1200 Series HPLC equipped with an Eclipse Plus XDB-C18 column with 4.6 × 150 mm dimensions and 5 µm particle size. The salicylic acid method employed an isocratic method of 30% acetonitrile and 70% pH 2.8, 10 mM H_3PO_4 with a flow rate of 1.0 mL min^{-1}. Detection was accomplished using a fluorescence detector with excitation and emission wavelengths set to 320 nm and 410 nm, respectively. The typical retention time of salicylic acid in the system was approximately 6 min. The phenol method employed an isocratic method of 30% acetonitrile and 70% pH 2.8, 10 mM H_3PO_4 with a flow rate of 1.0 mL min^{-1}. Detection was accomplished using a fluorescence detector with excitation and emission wavelengths set to 260 nm and 310 nm, respectively. The typical retention time of phenol in the system was approximately 5 min.

Irradiation experiments

A Rayonet RPR-100 (Southern New England Ultraviolet Company) was used for irradiations, employing either 254 or 320 nm lamps. The 254 nm lamps emit light ranging from 249 nm

to 258 nm. Quantum yield calculations for experiments using 254 nm lamps were treated as monochromatic. The 320 lamps emit light ranging from 270 to 400 nm, with maximum emission at 313 nm. Quantum yield calculations for experiments using 320 nm lamps were treated as polychromatic. Lamp spectra overlaid with absorption spectra of the Sens can be found in the Figure 2. The Rayonet RPR-100 employs a fan to control temperature. Lamp spectra overlaid with absorption spectra of the probe compounds (benzene and benzoic acid) and their hydroxylated products (phenol and salicylic acid) can be found in the Figure 3. The Rayonet RPR-100 employs a fan to control temperature. Irradiance spectra of the lamps were collected using a spectroradiometer and can be found in the Figures 2 and 3.

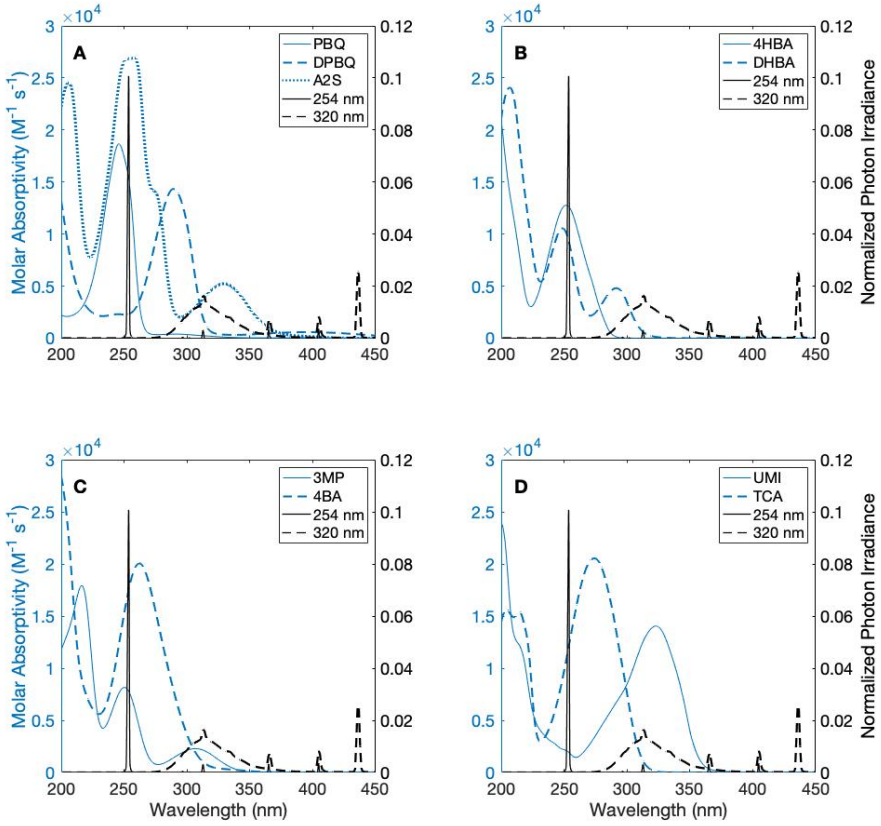

Figure 2. Molar absorptivity of sensitizers on the left y-axis and normalized (total area = 1) lamp spectra on the right y-axis. A: Quinones, B: Hydroxybenzoic acids, C: Aromatic ketones, and D: Other triplet forming species.

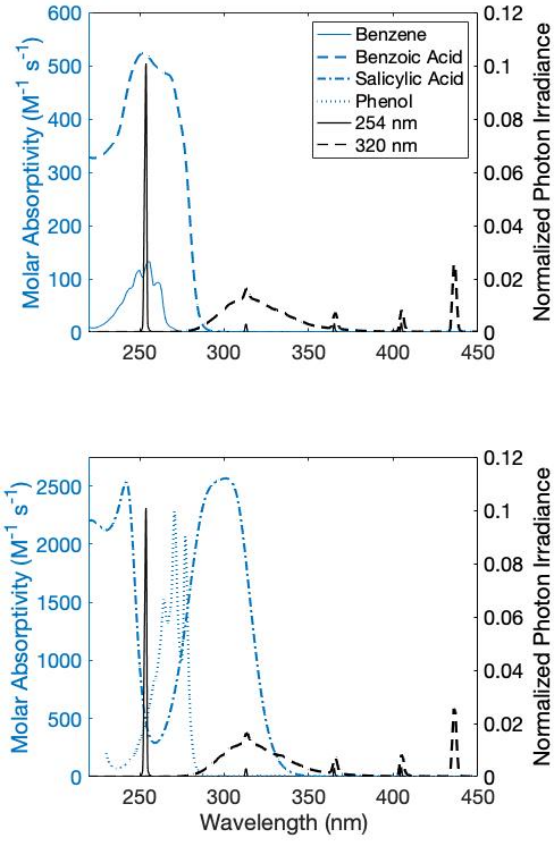

Figure 3. Molar absorptivity of probes (benzene and benzoic acid) and hydroxylated probes (phenol and salicylic acid) on the left y-axis and normalized (total area = 1) lamp spectra on the right y-axis. Benzene and phenol molar absorptivity data is from literature.[44]

Photon irradiance was quantified daily using chemical actinometry: Uridine actinometry was used for 254 nm irradiations and *p*-nitroanisole/pyridine (PNA/PYR) actinometry was used for 320 nm irradiations. Uridine was used as an actinometer following the procedure from literature.[45] A stock uridine solution of 1.2 μM was prepared in 1 mM phosphate buffer (pH 7.0). This solution was irradiated and at regular time intervals vials were withdrawn from the reactor and the uridine concentration measured spectrophotometrically using the molar extinction coefficient of 8593 M^{-1} cm^{-1} at λ=262 nm. Photon irradiance was calculated according to the following equation with the irradiance typically being about 1.7×10^{-8} Einstein cm^{-2} s^{-1},

$$I_{0,254nm} = \frac{k'[\text{uridine}]_0 l}{1000\Phi_{\text{uridine}}(1 - 10^{-\varepsilon_{uridine}[[\text{uridine}]_0]l})} \quad (1)$$

where $I_{0,254nm}$ is the photon irradiance (Einstein cm^{-2} s^{-1}) for the 254 nm lamps, which are treated as a monochromatic light source, k' is the observed first-order rate constant for uridine decay (s^{-1}), [uridine]$_0$ is the initial concentration of uridine (M), l is the path length, Φ_{uridine} is the quantum yield for uridine photodegradation (0.020), and $\varepsilon_{\text{uridine}}$ is the molar extinction coefficient for uridine (10185 M^{-1} cm^{-1}) at 254 nm.[45]

p-Nitroanisole (PNA) / pyridine (PYR) actinometry was used following an established procedure using a solution containing 10 μM PNA and 5 mM PYR.[46] The disappearance of PNA was monitored throughout irradiation time using HPLC for detection, employing 50% 10 mM phosphoric acid/50% acetonitrile mobile phase with UV detection at 300 nm. The typical retention time of PNA in the system was approximately 2.3 min. These data were fitted to a first-order kinetic model. Eqs 2 and 3 were used to calculate the photon irradiance, with the irradiance typically being about 1.3×10^{-7} Einstein cm^{-2} s^{-1},

$$I_{0,320nm} = \frac{k'[PNA]_0 l}{1000\Phi_{PNA}\sum_{\lambda}(1 - 10^{-\varepsilon_{PNA,\lambda}[PNA]_0 l})} \quad (2)$$

$$\Phi_{\text{PNA}} = 0.29[\text{PYR}] + 0.00029 \quad (3)$$

where $I_{0,320\text{nm}}$ is the photon irradiance (Einstein cm^{-2} s^{-1}) for the 320 lamps, which emit light over a spectrum seen in Figures 2 and 3, k' is the observed first-order rate constant for PNA decay (s^{-1}), [PNA]$_0$ is the initial concentration of PNA (M), l is the path length, Φ_{PNA} is the PNA quantum yield and is calculated using eq 3, and $\varepsilon_{\text{PNA},\lambda}$ is the molar extinction coefficient for PNA over the wavelengths emitted by the 320 nm lamps.[46]

Irradiation experiments at 254 nm were performed with 1 mM benzoic acid as the probe compound and experiments at 320 nm were performed using 3 mM benzene as the probe

compound. At these concentrations the probe compounds act as rate of formation probes, rendering the fraction of conversion of the probes to be negligible. For experiments performed using 254 nm lamps the concentration of Sens was adjusted to be optically matched at an initial optical density of 0.3. Concentrations of Sens in experiments normalizing absorbance to 0.3 ranged from approximately 10 – 100 μM. Solution temperature was not controlled due to the short irradiation times required with little temperature variation, between 23 and 28 ºC. For experiments performed using 320 nm lamps Sens concentrations were 20 μM. Longer irradiation times were required for 320 nm experiments and a shift in temperature was observed as a result of longer irradiation time. For this reason, prior to experimentation the solution temperature was adjusted to 30 ± 3 ºC using a water-jacketed petri dish, which is the steady-state temperature of the photochemical reactor.

Two corrections were made to experimental data. First, because benzoic acid absorbs strongly at 254 nm (Figure 3), the light screening factor for these experimental solutions was calculated and quantum yields were corrected for light screening following the procedure by Wenk et al. (2011).[4] The equation used for these calculations is as follows,

$$S_{\lambda,PC,Sens} = \frac{1 - e^{-2.303\left(\varepsilon_{\lambda,PC}[PC] + \varepsilon_{\lambda,Sens}[Sens]\right)l}}{2.303\left(\varepsilon_{\lambda,PC}[PC] + \varepsilon_{\lambda,Sens}[Sens]\right)l} \qquad 4$$

where $\varepsilon_{\lambda,PC}$ and $\varepsilon_{\lambda,Sens}$ are the molar extinction coefficients for the PC and Sens in M^{-1} cm^{-1} and [PC] and [Sens] are the concentrations of PC and Sens in M. Light screening factors for solutions containing Sens normalized to absorbance of 0.3 were 0.43. Using benzene with the 320 nm lamps did not present the same issue, as benzene does not absorb strongly in the wavelength range emitted by these lamps, shown in Figure 3. Second, for all experiments with Sens, rates of formation of the hydroxylated probe compound were corrected for the production of the hydroxylated probe compound from the direct photolysis of the probe compound itself. Additionally, control experiments were performed with DHBA to determine whether direct photolysis of DHBA results in

salicylic acid, chromatograms for HPLC analysis of these experimental solutions are shown in Figure 4. This data shows that the direct photolysis of DHBA does not produce salicylic acid and, therefore, will not affect the quantum yield results.

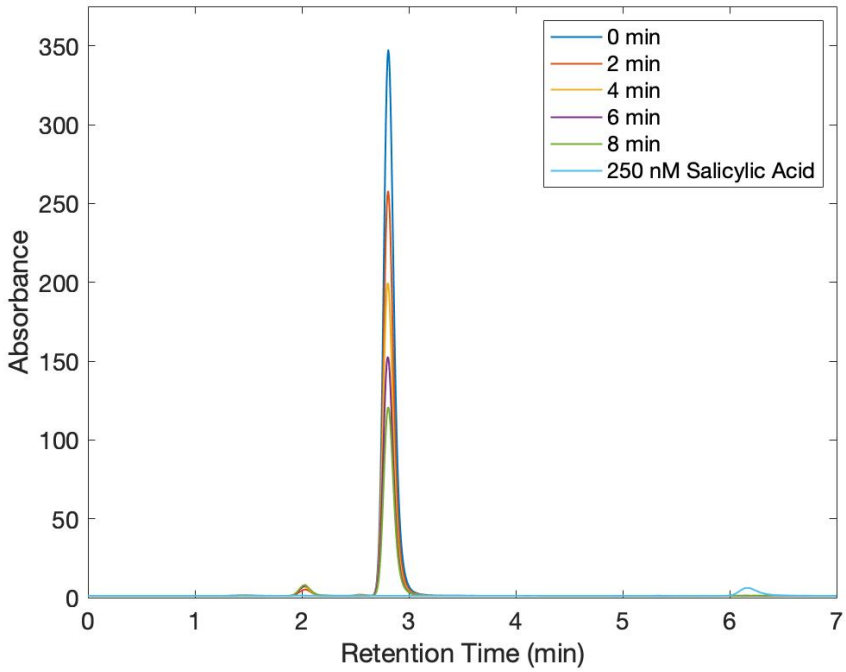

Figure 4. Chromatograms for irradiation of DHBA with 254 nm lamps at 0, 2, 4, 6, and 8 minutes. Shown in light blue is a 250 nM salicylic acid standard.

It is important to note that experimental limitations required use of different probe compound at 254 nm and 320 nm irradiation. Specifically, salicylic acid absorbs in the wavelength range emitted by the 320 nm lamps (Figure 3) and undergoes non-negligible direct photolysis (Figure 5), which precluded use of 320 nm lamps with benzoic acid as a probe compound. At 254 nm, benzoic acid and Sens screen the majority of the incoming light, minimizing direct photolysis of the salicylic acid photoproduct which is in the nM concentration range. The hydroxylated product of benzene (phenol) does not absorb at 320 nm (Figure 3).

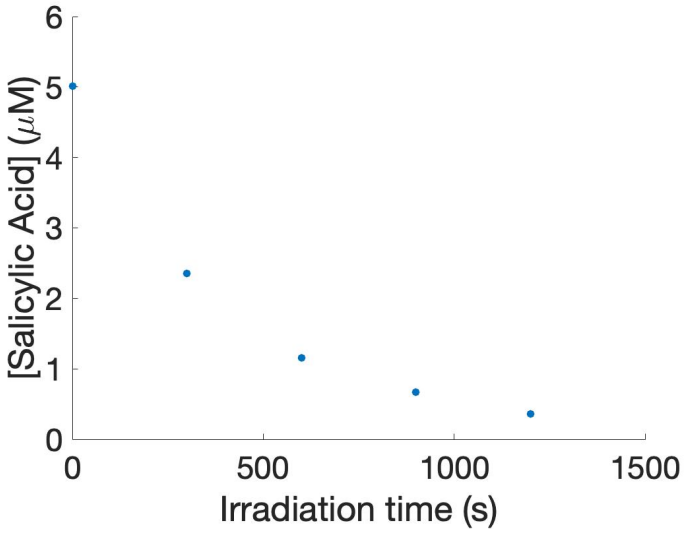

Figure 5. Direct photolysis of salicylic acid at 320 nm results in rapid first order decrease in salicylic acid concentration.

Methanol was added as a quencher in some experiments to assess whether or not the •OH-like species reacts with methanol similarly to •OH. In these experiments, HPLC grade methanol was spiked into solutions prior to irradiation at concentrations ranging between 0 and 0.1 M. Methanol reacts with •OH with a second-order reaction rate constant of 9.7×10^8 M^{-1} s^{-1}.[7] It is hypothesized that the reaction between methanol and other hydroxylating species to be different than that of •OH because hydroxyl radicals are non-selective and react with many molecules at near diffusion-controlled rates. A similar method was used in a study of DOM photochemistry by Leresche et al. (2021).[47]

Reaction pathways involving methanol or triplet quinones have been shown to produce superoxide, a fraction of which will dismutate to H_2O_2, which can undergo direct photolysis to form •OH.[48–51] Calculations were performed to estimate the rate of formation of •OH from these pathways considering both 254 and 320 nm irradiation. Estimated rate of formation of •OH from H_2O_2 photoylsis for varying concentrations of H_2O_2 under 254 and 320 nm irradiation conditions were calculated using the following equation

$$R_{\bullet OH} = \Phi_{\bullet OH}[H_2O_2]\sum_{\lambda} k_{Sens-a} \quad (5)$$

where k_{Sens-a} was calculated using eq 7 and values for ε_{H2O2} and $\Phi_{\bullet OH}$ for H_2O_2 photolysis were found in literature.[50,52] The concentration of H_2O_2 was estimated using experimental data from other studies.[48,49] The highest resulting value being on an order of 10^{-12} M s^{-1} when using a [H_2O_2] of 20 μM. This value is ~2 – 3 orders of magnitude lower than the rates of formation observed in this study. Other estimated values for the rate of formation of •OH from H_2O_2 photoylsis vary based on the concentration of H_2O_2, as seen in Table 2. Based on these calculations, H_2O_2 is not expected to contribute significantly to observed rates of formation of hydroxylated probe compounds.

Table 2. Rate of formation of •OH from H_2O_2 photolysis, calculated using eq 5.

$[H_2O_2]$	$R_{\bullet OH,254nm}$ (M s^{-1})	$R_{\bullet OH,320nm}$ (M s^{-1})
100 nM**	7.6×10^{-15}	9.1×10^{-15}
1000 nM**	7.6×10^{-14}	9.1×10^{-14}
20 M*	1.5×10^{-12}	1.8×10^{-12}

*Approximate concentration of Sens used in photochemistry experiments reported in this study.
**Within concentration range of measured H_2O_2 from photochemistry experiments with DOM and quinones.[48,49]

Quantum Yield Analysis

In order to compare the photoreactivity of Sens, apparent •OH quantum yields were calculated. Quantum yields were calculated for Sens in benzoic acid with 254 nm light and benzene with 320 nm light systems. Apparent quantum yields were calculated as described by the following equation,

$$\Phi_{OH} = \frac{R_{\bullet OH}}{k_{Sens-a}[Sens]} \quad (6)$$

where $R_{\bullet OH}$ is the rate of formation of hydroxylating species in M s^{-1}, k_{Sens-a} is the specific rate of light absorption by Sens in s^{-1}, and [Sens] is Sens concentration in M. The specific rate of light absorption of Sens was calculated using eq 7.

$$k_{\mathrm{Sens}-a} = 1000 E^0_{\mathrm{p,total}} \sum_{\lambda} \frac{\rho_\lambda \varepsilon_{\lambda,Sens}\left(1 - 10^{-(\varepsilon_{\lambda,Sens}[\mathrm{Sens}]+\varepsilon_{\lambda,PC}[\mathrm{PC}])l}\right)}{(\varepsilon_{\lambda,Sens}[\mathrm{Sens}] + \varepsilon_{\lambda,PC}[\mathrm{PC}])l} \qquad 7$$

In eq 7, $E^0_{\mathrm{p,total}}$ is the photon irradiance of the Rayonet photoreactor in Einstein cm^{-2} s^{-1}, ρ_λ is the relative spectral photon irradiance, $\varepsilon_{\lambda,Sens}$ is the molar absorption coefficient at the wavelength λ of the Sens in M^{-1} cm^{-1}, [Sens] is Sens concentration in M, $\varepsilon_{\lambda,PC}$ is the molar absorption coefficient at the wavelength λ of the probe compound in M^{-1} cm^{-1}, [PC] is the concentration of the probe compound in M, and l is the optical pathlength in cm. Additionally, $R_{\bullet\mathrm{OH}}$ is defined as follows,

$$R_{\bullet\mathrm{OH}} = \frac{R_{PC-OH}}{Y_{\bullet\mathrm{OH}}} \qquad 8$$

where R_{PC-OH} is the rate of formation of the hydroxylated probe compound and $Y_{\bullet\mathrm{OH}}$ is the yield for the reaction of •OH with the probe compound.

The yield for the reaction of other hydroxylating species with the probe compound, $Y_{\bullet\mathrm{OH-like}}$, is unknown, so for these calculations, $Y_{\bullet\mathrm{OH}}$ was used for all Sens. A reasonable hypothesis about whether $Y_{\bullet\mathrm{OH-like}}$ is less than or greater than $Y_{\bullet\mathrm{OH}}$ cannot be made without more information about the identity of the •OH-like intermediate and the mechanism by which it reacts with probe compounds. Additionally, this difference is difficult to quantitatively constrain due to the unknown quantum yield for the production of other hydroxylating species from Sens (apart from the use of probe compounds). Therefore, the quantum yields calculated in this study simply use $Y_{\bullet\mathrm{OH}}$ as a benchmark for the expected value of $Y_{\bullet\mathrm{OH-like}}$. Even for •OH, a wide variety of yields exist in the literature for different arenes (e.g., ~0.3-0.9 for $Y_{\bullet\mathrm{OH}}$ of phenol from benzene), which may also be sensitive to solution conditions.[53–57] $Y_{\bullet\mathrm{OH}}$ for the reaction of •OH with benzene to produce phenol, two more recent studies, Sun et al. (2014) and McKay and Rosario-Ortiz (2015), determined this yield to be 0.693 ± 0.022 and 0.63 ± 0.07, respectively.[20,58] These values are in good agreement with each other and fall within the aforementioned range for this parameter. For

this study the value determined by McKay and Rosario-Ortiz (2015), which utilized similar experimental conditions was used. $Y_{\bullet OH}$ for the reaction of •OH with benzoic acid to form salicylic acid a value of 0.155 was used.[41]

Methanol Quenching Model

Methanol quenching was modeled by eq 9, where f is the fraction of •OH reacting with the probe compound,

$$f = \frac{k_{PC,\bullet OH}[PC]}{k_{MeOH,\bullet OH}[MeOH] + k_{PC,\bullet OH}[PC] + k_{Sens,\bullet OH}[Sens]} \quad 9$$

where $k_{PC,\bullet OH}$, $k_{MeOH,\bullet OH}$, and $k_{Sens,\bullet OH}$ are the second order rate constants for respectively the probe compound, Sens, and methanol (MeOH) with •OH in M^{-1} s^{-1}, respectively. [PC], [Sens], and [MeOH] are the concentrations of respectively the probe compound, Sens, and MeOH in M.

RESULTS

Production of Hydroxylating Species from Model Sensitizers

The formation of hydroxylating species (•OH and •OH-like species) from Sens was assessed using two different probe compounds with two irradiation wavelengths, benzoic acid with 254 nm irradiation and benzene with 320 nm irradiation. Figure 6 shows the results for the experiments performed using benzoic acid with 254 nm irradiation. Figure 7 shows results for the experiments using benzene with 320 nm irradiation. Formation rates for the data in these figures can be found in the Table 3. All samples were interpreted as linear with respect to the formation of the hydroxylated probe compound with one exception: A2S with 320 nm irradiation using benzene as the probe compound because the production of phenol is clearly nonlinear (Figure 7B). Direct photolysis controls revealed that benzoic acid photolysis produces salicylic acid with a formation rate equal to 1.4 ± 0.08 nM s^{-1}. Of the examined Sens, irradiation of quinones and hydroxybenzoic acids produced greater rates of salicylic acid formation (> 3.0 nM s^{-1}) than direct photolysis of benzoic acid, indicating that these Sens have a hydroxylating capacity. Irradiation of quinones produced salicylic acid at rates between 5.9 and 26 nM s^{-1}, whereas irradiation of hydroxybenzoic acids produced salicylic acid at rates between 3.0 and 3.4 nM s^{-1}. Conversely, the formation of salicylic acid in samples containing aromatic ketones and other triplet forming species was within the range of the direct photolysis control, suggesting that these Sens had a minimal hydroxylating capacity, if any.

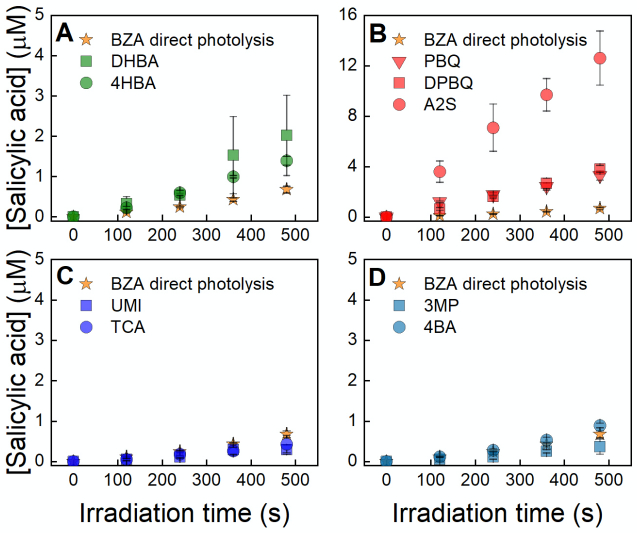

Figure 6. Production of salicylic acid with respect to time from the photolysis of Sens in the presence of 1 mM benzoic acid, irradiated at 254 nm for 8 minutes. All samples were adjusted to pH 7.0 ± 0.1. The concentration of Sens was adjusted to be optically matched at an initial optical density of 0.3. Each subplot displays benzoic acid (BZA) direct photolysis data. **A**: 2,4-Dihydroxybenzoic acid (DHBA), 4-Hydroxybenzoic acid (4HBA), **B**: *p*-Benzoquinone (PBQ), 2,6-Dimethoxy-*p*-bezoquinone (DPBQ), Anthraquinone-2-sulfonate (A2S), **C**: Umbelliferone (UMI), *trans*-Cinnamic acid (TCA), and **D**: 3-Methoxyacetophenone (3MP), 4-Benzoylbenzoic acid (4BA).

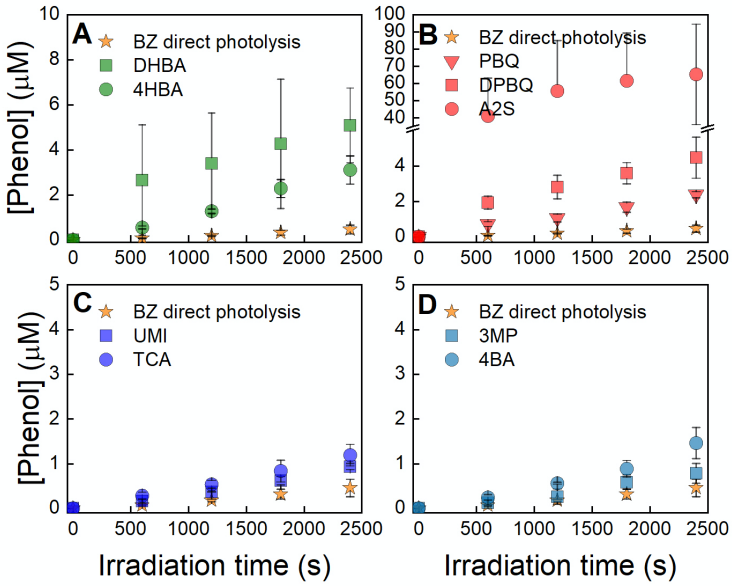

Figure 7. Production of phenol with respect to time from the photolysis of 20 μM Sens in the presence of 3 mM benzene, irradiated at 320 nm for 40 minutes. All samples were adjusted to pH 7.0 ± 0.1. Each subplot displays benzene (BZ) direct photolysis data. **A**: 2,4-Dihydroxybenzoic acid (DHBA), 4-Hydroxybenzoic acid (4HBA), **B**: *p*-Benzoquinone (PBQ), 2,6-Dimethoxy-*p*-benzoquinone (DPBQ), Anthraquinone-2-sulfonate (A2S), **C**: Umbelliferone (UMI), *trans*-Cinnamic acid (TCA), and **D**: 3-Methoxyacetophenone (3MP), 4-Benzoylbenzoic acid (4BA).

Similar to the results obtained with benzoic acid at 254 nm, direct photolysis of benzene leads to its photohydroxylation, forming phenol (0.19 ± 0.04 nM s^{-1}, Table 3). As shown in Figure 7 and Table 3, all Sens irradiated in the presence of benzene produced phenol at rates greater than could be accounted for by direct photolysis alone (between 0.39 and 2.2 nM s^{-1}). Quinone and hydroxybenzoic acid Sens had rates of phenol formation sufficiently higher than that of the direct photolysis of benzene (all greater than 0.95 nM s^{-1}), compared to the results obtained for the aromatic ketones, umbelliferone, or trans-cinnamic acid which were a maximum of 0.41 nM s^{-1} (for 4-benzoyl benzoic acid) greater than the rate of formation from benzene. All samples, except those containing A2S, were interpreted as linear with respect to the formation of phenol. In the case of A2S, the production of phenol was not linear, and the formation rate was not included in Table 3. This behavior can be attributed to the reaction of triplet A2S with phenol, as it has been previously

established that phenol is oxidized by A2S (E^{o*} = 2.28 V).[23] DPBQ may be able to oxidize phenol, but the reaction does not appear to occur significantly on the timeframe of the experiments. Lerescheet al. (2021) observed a small (10%) degradation of salicylic acid in irradiation experiments of DOM, which contains quinone moieties, on a relatively longer timeframe (4 hours) than the condition used in the present study.[47]

Table 3. List of formation rates (nM s^{-1}) of salicylic acid and phenol for experimental conditions 254 nm/benzoic acid and 320 nm/benzene, respectively. This data can be found in Figures 6 and 7 in the main text. ND = No data in the case of A2S because the formation of phenol is not linear.

Sensitizer	254 nm/Benzoic acid (nM s^{-1})	320 nm/Benzene (nM s^{-1})
PBQ	5.9 ± 0.46	0.95 ± 0.07
DPBQ	8.1 ± 0.46	2.2 ± 0.19
A2S	26 ± 1.73	ND
4HBA	3.0 ± 0.13	1.3 ± 0.13
DHBA	3.4 ± 0.83	1.9 ± 0.27
4BA	1.0 ± 0.05	0.60 ± 0.08
3MP	0.45 ± 0.10	0.43 ± 0.07
TCA	0.51 ± 0.13	0.39 ± 0.01
UMI	0.31 ± 0.11	0.49 ± 0.06
Direct photolysis of probe	1.4 ± 0.08	0.19 ± 0.04

Figure 7B shows that the yield of phenol from A2S photolysis is greater than the original concentration of A2S in solution. There are a few possible explanations for this behavior. One study found that the photodecomposition of anthraquinones is fully reversible in the presence of oxygen, while this is not true in the case of benzoquinones.[60,61] This catalytic process could be contributing to increased yields of hydroxylating species in the case of anthraquinones. Additionally, some studies have observed an increase in the production of superoxide and hydrogen peroxide from anthraquinone-2,6-disulfonate and 9,10-anthraquinone derivatives in the presence of an electron donor.[49,62] It is possible that benzene (which has an oxidation potential of ~2.2 V)[63] facilitates the catalytic production of hydrogen peroxide by continuously cycling A2S between reduced ($A2S^{\bullet-}$) and oxidized (A2S) states without forming other stable quinone photoproducts. In the

presence of an electron donor, if a higher concentration of hydrogen peroxide is formed an appreciable amount of •OH could then be formed from hydrogen peroxide photolysis. However, based on calculations using eq 5 shown in Table 2, this pathway is not expected to be a significant contributor to the production of •OH in the case of anthraquinone-2,6-disulfonate. However, that is not the anthraquinone sulfonate tested in this study and may not be entirely representative of the A2S photochemistry presented here. Ultimately, it is possible that a combination of pathways that produce hydroxylating species are contributing to the photochemical behavior of A2S observed in Figure 7B.

Overall, the data presented in Figures 6 and 7 indicate that quinones and hydroxybenzoic acids have a hydroxylating capacity. However, in contrast to the data from experiments using benzoic acid with 254 nm irradiation (Figure 6), experiments using benzene with 320 nm irradiation (Figure 7) show that the formation of phenol in systems containing aromatic ketones and other triplet forming species may not entirely be attributed to the direct photolysis of benzene. For the purposes of this study, aromatic ketones and other triplet forming species were not investigated further because their formation rates were barely outside of the uncertainties for the direct photolysis of benzene. Even if these Sens do participate in the production of hydroxylating species, it is to a much lesser extent than quinones and hydroxybenzoic acids.

Estimation of Quantum Yields for Model Sensitizers

Quantum yields were calculated for Sens (Table 4). The quantum yields for the 320 nm lamps are apparent quantum yields for the polychromatic lamps. There are two complicating factors for calculating the quantum yields for the Sens. First, because the yields of hydroxylated probe compound from the reaction of hydroxylating species other than •OH is unknown, the yield for the reaction of the probe compound with •OH ($Y_{\bullet OH}$) was used. It is expected that the reaction rate

constants of these •OH-like species are different than that of •OH, which reacts with benzene and benzoic acid at near diffusion-controlled rates.[7] For this reason, the data in Table 4 can be treated as estimates of the true quantum yield for these systems. Second, there is the issue of the concentration of Sens changing with irradiation time. To evaluate this second issue, solutions of only Sens were irradiated under the same conditions described above and the absorbance spectra of those solutions were measured at different irradiation times. Changes in concentration of Sens were observed in for quinones and hydroxybenzoic acids, which are the Sens that have been identified to have a hydroxylating capacity, at both wavelengths (Figures 8 and 9). Regarding quinones, PBQ rapidly photodegrades under both wavelength conditions and A2S and DPBQ undergo rapid photodegradation with 320 nm irradiation. For hydroxybenzoic acids, Figure 9 shows rapid photodegradation of DHBA at 320 nm. Quantum yields for these Sens at these wavelengths were not calculated.

Table 4. Quantum yields for the production of hydroxylating species using benzoic acid and benzene as probe compound and irradiating at 254 and 320 nm, respectively. Values represent average of at least triplicate measurements with error representing one standard deviation. Values assume a $Y_{\bullet OH}$ value of 0.63 and 0.15, equal to that of •OH, for benzene and benzoic acid, respectively. The quinones are highlighted in red and the hydroxybenzoic acids in blue to reflect the color code of Figure 1. ND = No quantum yield data for sensitizer because direct photodegradation of sensitizer occurred on a timescale too short for accurate quantum yield computation. Direct photodegradation data can be found in the Figures 8 and 9.

Model Sensitizer	Benzoic Acid (254 nm irradiation) ($\times 10^{-3}$)	Benzene (320 nm irradiation) ($\times 10^{-3}$)
p-Benzoquinone (PBQ)	ND	ND
Anthraquinone-2-sulfonate (A2S)	47 ± 1.2	ND
2,6-Dimethoxy-p-benzoquinone (DPBQ)	17 ± 0.55	ND
2,4-Dihydroxybenzoic acid (DHBA)	6.3 ± 0.28	ND
4-Hydroxybenzoic acid (4HBA)	5.4 ± 0.13	11 ± 0.91

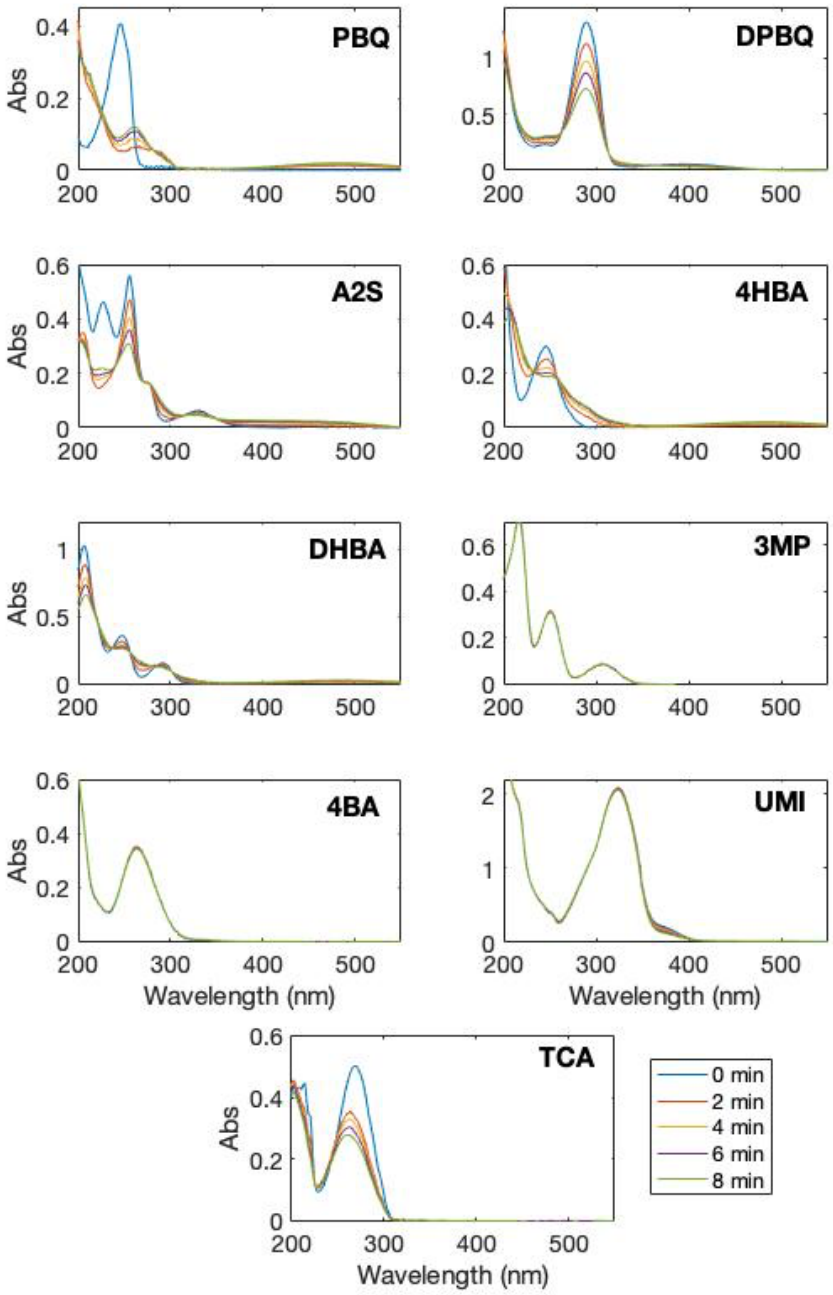

Figure 8. Absorbance spectra of Sens at 0-, 2-, 4-, 6-, and 8-minutes irradiation times, exposed to 254 nm lamps.

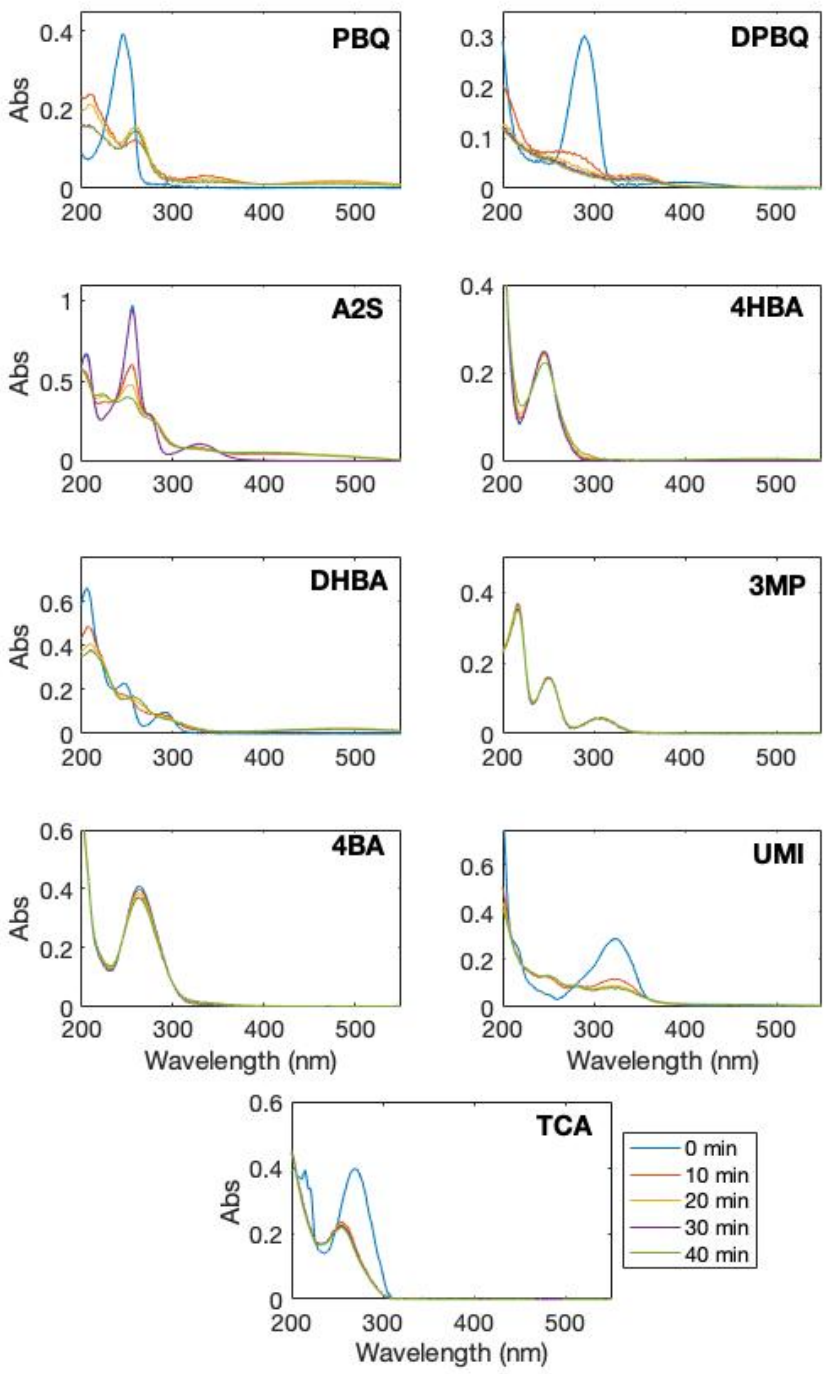

Figure 9. Absorbance spectra of Sens at 0-, 10-, 20-, 30-, and 40-minutes irradiation times, exposed to 320 nm lamps.

Interestingly, although quinone degradation is significant, the formation rate of the hydroxylated probe compounds is linear in all cases but one, where it is expected that triplet A2S is reacting with phenol (Figures 7B). One hypothesis is that the quinone and hydroxybenzoic acid photoproducts also have a hydroxylating capacity. For quinones, this was tested by running experiments with hydroquinone, a quinone photoproduct,[19] using 320 nm lamps with benzene as the probe compound. This experiment was performed employing the same conditions as with other Sens at this wavelength. These results can be found in the Figure 10. Production of phenol is observed in these experiments, indicating that hydroquinone has a hydroxylating capacity with a rate of formation of 1.1×10^{-9} M^{-1} s^{-1}, approximately an order of magnitude higher than the rate of formation of phenol from the direct photolysis of benzene, 1.94×10^{-10} M^{-1} s^{-1}. Based on these results, it is hypothesized that the quantum yields for quinones presented in this study are representative of the photochemistry of both quinones and quinone photoproducts, which could account for the linear rate of formation despite the fast photodegradation of quinones in these experimental conditions. The degradation of the hydroxybenzoic acids happens less rapidly than that of quinones but is still not negligible, especially in the case of DHBA with 320 nm irradiation. It is possible that the photoproducts of hydroxybenzoic acids also have a hydroxylating capacity, but the photoproducts of these compounds are not well established. Based on the photochemical behavior observed for hydroquinone, it is hypothesized that quantum yields presented in this study are estimations for the quantum yields for the formation of hydroxylating species from a combination of Sens and their photoproducts.

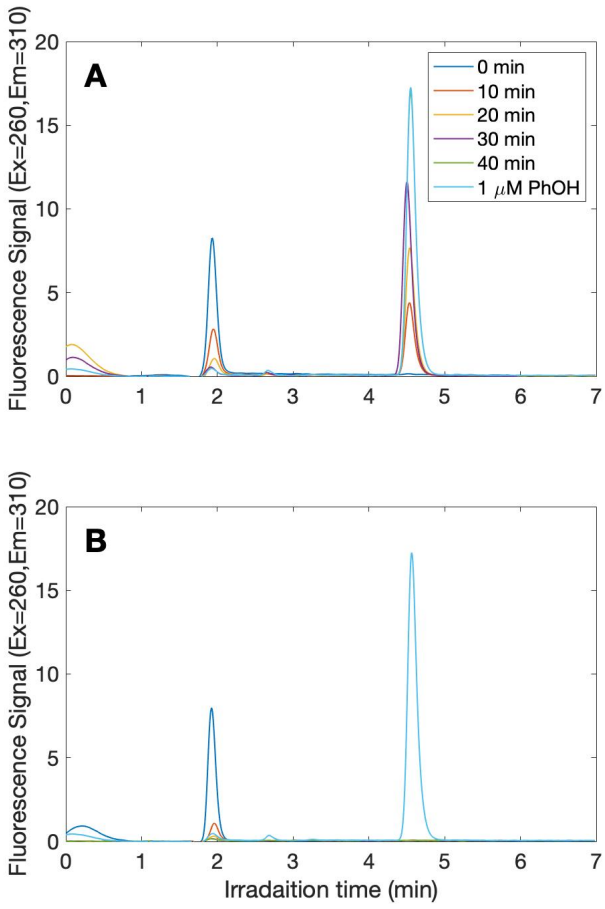

Figure 10. A: Chromatograms for detection of phenol from the photolysis of hydroquinone and PBQ using 320 nm with benzene as a probe compound. B: Chromatograms for direct photolysis of hydroquinone using the phenol method for HPLC analysis.

Quinone quantum yields at 254 nm for A2S and DPBQ were (47 ± 1.2) × 10^{-3} and (17 ± 0.55) × 10^{-3}, respectively. These values are ~1 order of magnitude lower than the quantum yield value reported by Gan et al. (2008), which is 0.37 ± 0.04.[19] This difference may be derived from the use of different probe compounds, benzoic acid used in this study and DMSO used by Gan et al. (2008). Notably, a number have studies have concluded that DMSO is not a suitable probe for detecting hydroxylating species produced from quinone photolysis.[37,40] One study did not detect a hydroxylating species from *p*-benzoquinone photolysis when using DMSO as a probe, while another did but attributed this to the direct reaction of the triplet quinone with DMSO.[37,40] Taken as

a whole, the existing data does not support the use of DMSO as a probe compound for the production of hydroxylating species from quinone photolysis. Consequently, the quantum yield measured by Gan et al. (2008) is questionable. Moreover, calculations performed to relate the absorbance by quinones in DOM to the quantum yields measured in this study validate the order of magnitude of the quantum yields presented here. For more information about these calculations, see the Environmental Implications section.

For hydroxybenzoic acids, variation in the quantum yields with wavelength was observed, $(5.4 \pm 0.13) \times 10^{-3}$ at 254 nm and $(11 \pm 0.91) \times 10^{-3}$ at 320 nm, for 4HBA (Table 4). There are two possible reasons for variation in quantum yields, wavelength dependence of the photochemistry and the use of different probe compounds. In a study by Sun et al. (2015),[22] variation in quantum yield with wavelength was observed to range from $(8.0 – 12.9) \times 10^{-3}$ over 290 – 320 nm for 2,4-dihydroxybenzoic acid and $(10.0 – 11.3) \times 10^{-3}$ over 280 – 290 nm for 4-hydroxybenzoic acid when using the same probe compound, indicating that the photochemical pathway by which hydroxylating species are produced from this class of Sens is wavelength dependent. Additionally, the resulting quantum yield of $(11 \pm 0.91) \times 10^{-3}$ for 4HBA using the 320 nm lamps (wavelength range 270 to 400 nm) is supports the result published by Sun et al. (2015), $(10.0 – 11.3) \times 10^{-3}$ over 280 – 290 nm, where benzene was also used as the probe compound.[22]

Even given the uncertainty in yield, there is benefit to presenting the data in terms of a quantum yield because this normalizes for differences in light absorption by the Sens. Additionally, calculating quantum yields for Sens also allows for the comparison to quantum yields measured for the formation of hydroxylating species from DOM.

Methanol Quenching

An important consideration to further understand the formation of hydroxylating species from DOM is the ability to differentiate between •OH and •OH-like species. Methanol was used as a quencher in order to investigate differences in the behavior of •OH and other hydroxylating species produced from quinones and hydroxybenzoic acids. These classes of Sens were selected based of data in Figures 6 and 7, which established that both classes of Sens have a hydroxylating capacity. Methanol reacts with •OH, with a rate constant of 9.7×10^8 M^{-1} s^{-1},[7] but the rate constant between methanol and other unknown hydroxylating species is unknown, although it is hypothesized to be different. Methanol quenching was modeled using the rate constant for •OH, represented as the fraction of •OH reacting with the probe compounds, f, as the concentration of methanol increases, represented by eq 9. Experimental data were compared to the model, f, to assess similarities between the behavior of •OH and other hydroxylating species.

Figure 11A shows normalized rates of formation for experiments performed using benzoic acid with 254 nm irradiation containing methanol and a Sens. Figure 11B shows normalized rates of formation for experiments performed using benzene with 320 nm irradiation containing methanol and a Sens. Methanol quenching of •OH produced from the photolysis of nitrate and nitrite was measured to confirm the modeled behavior of •OH.[64] In experiments containing nitrate (Figure 11A) and nitrite (Figure 11B), there is good agreement between observed and calculated quenching (i.e., f calculated via eq 9), considering the range of reported values for the rate constant of the reaction between •OH and methanol varies by about 20%.[7] Conversely, measured quenching for both quinones and hydroxybenzoic acids exhibited stark and inconsistent differences with calculated quenching in the two different probe/wavelength systems. For DHBA (a hydroxybenzoic acid hypothesized to produce free •OH) with benzoic acid and 254 nm irradiation, there is

incomplete quenching of the production of salicylic acid with increasing concentrations of methanol (Figure 11A, green circles). Conversely, for this same Sens but using benzene with 320 nm irradiation, methanol quenches the production of phenol to a greater degree than that modeled by •OH (Figure 11B, green circles). Considering quinones, when using PBQ and A2S as the Sens, no quenching of salicylic acid production by methanol was observed in samples using benzoic acid with 254 nm irradiation. However, when using benzene with 320 nm irradiation, PBQ exhibited quenching of the formation of phenol that was similar to that of •OH (Figure 11B, cyan circles).

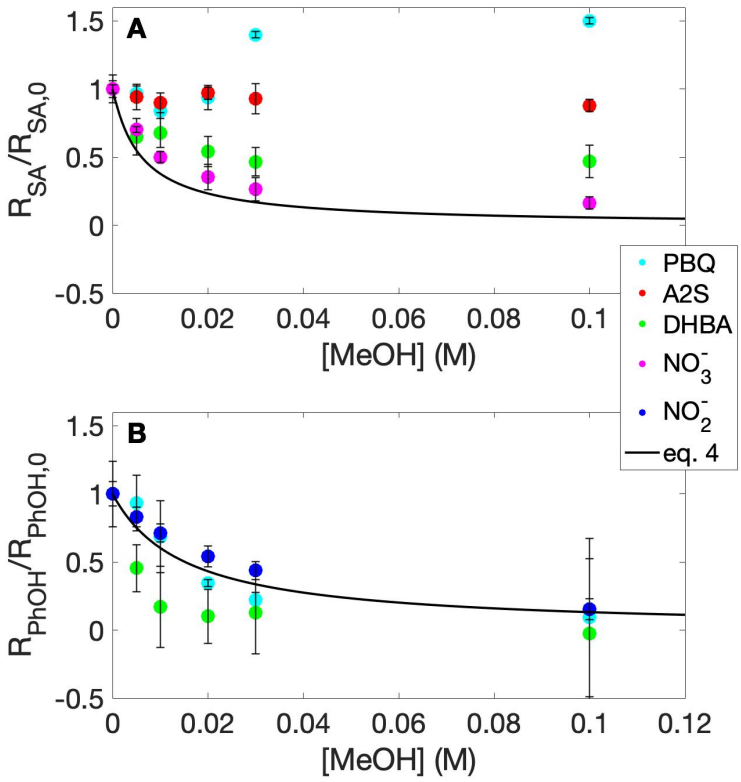

Figure 11. Effect of addition of methanol (•OH quencher) on the production of the hydroxylated probe compound. Left axis, normalized experimental rates of formation for the photolysis of 20 µM p-benzoquinone (PBQ), 20 µM anthraquinone-2-sulfonate (A2S), 20 µM 2,4-dihydroxybenzoic acid (DHBA), and 6 mM nitrate (NO_3^-) with a probe compound in the presence of 0, 0.005, 0.01, 0.02, 0.03, 0.1 M methanol. A: 1 mM benzoic acid as probe compound, 254 nm lamps. B: 3 mM benzene as probe compound, 320 nm lamps.

DISCUSSION

The goal of this work is to further understand the formation of •OH and other hydroxylating species from DOM. These results build on prior work that has established that quinones and hydroxybenzoic acids have a hydroxylating capacity,[19,21,22,34,37,42]. Aromatic ketones were selected to account for a class of sensitizers that are responsible for a portion of reactive triplet species in DOM and the other triplet forming species were selected to account for other triplet forming moieties that might be found in DOM. Aromatic ketones and other triplet forming species were two classes of sensitizers were expected to be negative controls for the production of hydroxylating intermediates.

Hydroxylating capacities of model sensitizers

Data in Figures 6 and 7 are supportive of previous studies indicating that quinones and hydroxybenzoic acids have a hydroxylating capacity. One previous study has reported the detection of •OH from the photolysis of hydroxybenzoic acids.[22] In this case, methane quenching experiments were supportive that the hydroxylating species responsible was free •OH. While several mechanisms were postulated,[22] no single mechanism has been established for the production of •OH from hydroxybenzoic acids.

The production of hydroxylating species from quinones has been studied more extensively than that of hydroxybenzoic acids. Studies have shown that the hydroxylating species produced by quinone photolysis is not •OH, but an •OH-like species proposed to be a triplet quinone – water exciplex.[21] Other studies suggest that if triplet quinones do form an exciplex with water, this species proceeds directly to other photochemical degradation products of quinones, unless there is sufficient concentration of other reactive compounds.[19,37,42] Additionally, previous work indicated that the quantum yield for the formation of phenol from benzene in the presence of PBQ had an

activation energy near zero.[20] In this case, this behavior was attributed to a multi-step process involving an exciplex.

Although data in Figures 7C and 7D could be taken as support that aromatic ketones and other triplet forming species have a hydroxylating capacity, it is hypothesized that this is not the case for two reasons. First, to the best of our knowledge there is no known photochemistry for aromatic ketones and the other triplet forming Sens that would lead to •OH or other hydroxylating species. Although prior studies have indicated that species having a very high one electron reduction potential (e.g., A2S) are capable of oxidizing hydroxide to from •OH,[10,23,65] the aromatic ketones and other triplet forming species in this study (Figure 1) have lower one electron reduction potential than A2S. Second, these data are not in agreement with the data from experiments using benzoic acid with 254 nm irradiation where salicylic acid formation was attributed solely to the direct photolysis of benzoic acid. Because the rates of formation for aromatic ketones (maximum of 2.7 nM s^{-1} for 4BA) and other triplet forming species (maximum of 2.4 nM s^{-1} for UMI) are at least a factor of two lower than that of the quinones (minimum of 4.8 nM s^{-1} for PBQ) and hydroxybenzoic acids (minimum of 6.2 nM s^{-1} for DHBA) and the formation is thought to be dependent on the probe compound and irradiation wavelength, for the purposes of this study, they will not be considered significant contributors to the overall production of hydroxylating species from DOM. Overall, the data displayed in Figures 6 and 7 is consistent with previous publications, confirming the presence of hydroxylating species from the photolysis of quinones and hydroxybenzoic acids.[19–22,35,42]

Methanol quenching: Hydroxybenzoic acids

There are a few possible explanations for behavior observed in the DHBA methanol quenching data (Figure 11). One is that the hydroxylating species produced from the photolysis of DHBA

is not •OH (in contrast with a study by Sun et al. (2015))[22] and this •OH -like species has rate constants with benzene, benzoic acid, and methanol that are different than •OH, resulting in a trend in the methanol quenching data that differs from that of •OH. Interestingly, if this •OH-like species has a rate constant with benzene that is an order of magnitude lower than that of •OH, 7.80×10^8 M^{-1} s^{-1} instead of 7.80×10^9 M^{-1} s^{-1}, then the experimental behavior of this hydroxylating species in the presence of benzene and methanol would match the model represented by eq 9, this is shown in Figure 12. However, not only is this hypothesis at odds with data reported by Sun et al. (2015)[22] that indicated that the photolysis of hydroxybenzoic acids produces free •OH, but it also only explains the behavior of DHBA in systems using benzene with 320 nm irradiation, not for benzoic acid with 254 nm irradiation. Sun et al. (2015)[22] used different quenchers and probe compound to determine whether the hydroxylating species detected was free •OH than those that were used in our study, including methane as a probe compound selective for •OH and formate as a competitor with benzene, which could be responsible for the conflicting results.[22]

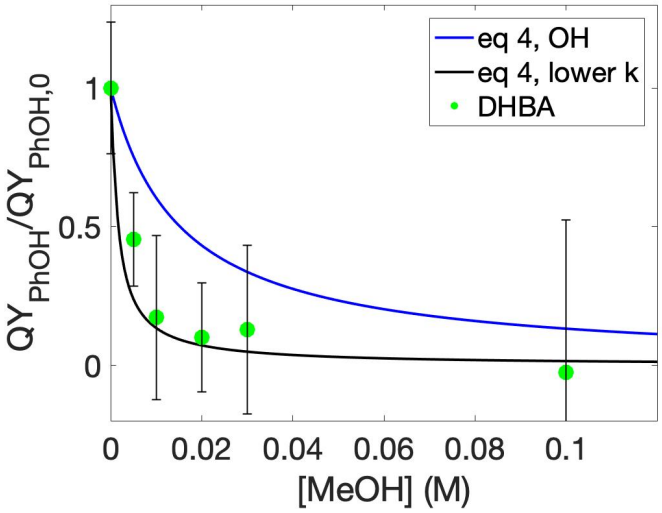

Figure 12. DHBA methanol quenching data in the system using benzene and 320 nm irradiation, compared to the model, eq 9 (main text), using two different values for $k_{PC,\bullet OH}$. In blue is the model where the rate constant for •OH was employed, in black is the model where a rate constant an order of magnitude lower than that of •OH, and in green is the methanol quenching data for DHBA.

Another possible explanation for the behavior in systems containing DHBA is that there are other photochemical pathways contributing to the formation and quenching of salicylic acid and phenol. One possible pathway that was tested, relevant to the use of benzoic acid with 254 nm irradiation, is production of salicylic acid from the direct photolysis of DHBA (Figure 4). If salicylic acid was being produced from the direct photolysis of DHBA as well as the reaction of the hydroxylating intermediate, that could explain the incomplete quenching of the formation of salicylic acid by methanol. However, no formation of salicylic acid was observed from the direct photolysis of DHBA (Figure 4), so the incomplete quenching of salicylic acid from the photolysis of DHBA is unaccounted for. Overall, the conflicting results described in Figure 11 demonstrate that methanol cannot distinguish between OH and OH-like species from hydroxybenzoic acids.

Methanol quenching: Quinones

Quinones (PBQ and A2S) exhibited no quenching of salicylic acid formation in experiments using benzoic acid with 254 nm irradiation upon methanol addition. Conversely, when using

benzene with 320 nm irradiation, the quenching of phenol formation from quinone photolysis was similar to quenching observed for known free •OH sources (Figure 11). There are a few possible explanations for this behavior. One hypothesis for the difference in the 254 nm and 320 nm quenching data for quinones is that there are different hydroxylating intermediates being produced at the two wavelengths, one of which does not react with methanol, resulting in the absence of quenching behavior. It is possible that at 254 nm the hydroxylating species produced from quinone photolysis is the •OH-like species and that this species is not quenched by methanol and that at 320 nm •OH is produced, which has a well-known rate constant with methanol.[7] One study that utilized EPR to investigate the reactivity of t-butanol with •OH produced from H_2O_2 and from PBQ photolysis observed that t-butanol was much more effective at reacting with •OH produced from H_2O_2 than •OH produced from PBQ photolysis, leading to the conclusion that the hydroxylating species observed in the EPR spectra is not •OH.[37] This study supports the hypothesis that alcohols react more slowly with •OH-like species than with •OH and that differences in the methanol quenching data shown in this study could be attributed to the presence of different hydroxylating species at the two wavelengths tested.

The second hypothesis is that the lack of quenching in the system using benzoic acid with 254 nm irradiation is due to the formation of salicylic acid from one-electron oxidation of benzoic acid by the triplet quinone, with the sum of the production from the hydroxylating species and the one-electron oxidation of benzoic acid by the triplet quinone. However, the oxidation potential of benzoic acid is 2.56 V[63] and the reduction potential of triplet PBQ is 2.42 V,[10] meaning if this reaction does occur it is happening relatively slowly. Additionally, if the formation of salicylic acid in these experimental conditions is due to the reaction of triplet quinones and the hydroxylating intermediate reacting with benzoic acid it is expected that there would still be some decrease

in the quenching trend in Figure 11, but this was not observed. For the two reasons listed previously, it is not expected that this is a likely explanation for the conflicting quenching behavior of quinones observed in Figure 11.

It is important to note that studies have shown that the photoreduction of triplet quinones happens in the presence of hydrogen donors, such as alcohols.[37] The reaction between triplet quinones and methanol is thought to produce a carbon centered radical, which can then react with ground state quinone to form formaldehyde.[37] The formation of formaldehyde was not measured in this study. To assess the contribution of methanol to reaction pathways of triplet quinone a calculation for the fraction of triplet quinone reacting with methanol in a system containing water, benzoic acid, methanol, and oxygen was performed using eq 10 and a figure displaying this data is presented in Figure 13, using the following rate constants. The rate constant for the reaction of triplet p-benzoquinone and oxygen is reported to be 2×10^9 M^{-1} s^{-1} and the rate constant for the reaction between triplet p-benzoquinone and methanol is reported to be 4.2×10^7 M^{-1} s^{-1}.[37] The rate constant of triplet methyl-p-benzoquinone with water has been estimated to be 7.3×10^4 M^{-1} s^{-1}.[19] The rate constant for the reaction between benzoic acid and triplet quinones has not been quantified, so eq 10 was calculated using values for k_{BA} ranging from 10^4 – 10^9 M^{-1} s^{-1} to assess the potential effect of this reaction.

$$f = \frac{k_{\mathrm{MeOH,3PBQ*}}[\mathrm{MeOH}]}{k_{\mathrm{MeOH,3PBQ*}}[\mathrm{MeOH}] + k_{\mathrm{BA,3PBQ*}}[\mathrm{BA}] + k_{\mathrm{H2O,3PBQ*}}[\mathrm{H_2O}] + k_{\mathrm{O2,3PBQ*}}[\mathrm{O_2}]} \qquad 10$$

In eq 10 $k_{\mathrm{MeOH,3PBQ*}}$, $k_{\mathrm{BA,3PBQ*}}$, $k_{\mathrm{H2O,3PBQ*}}$, and $k_{\mathrm{O2,3PBQ*}}$ are the rate constants for the reactions between triplet PBQ and MeOH, benzoic acid (BA), H_2O, and O_2, respectively.

According to Figure 13, at methanol concentrations lower than 0.03 M approximately 20% or less of triplet quinone reacts with methanol. At the highest concentration of methanol, 0.1 M, no more than 50% of the triplet quinone reacts with methanol, depending on the rate constant for

the reaction of benzoic acid and the triplet quinone. It is possible that complex chemistry involving methanol reactivity with triplet quinones in the presence of benzoic acid is contributing to a fraction of the lack of quenching observed in Figure 11A. Ultimately, the conflicting quenching trends for quinones, the use of different probes at the two wavelengths used in this study, and the possibility of the reaction of methanol with triplet quinones leave the question of the chemistry of the hydroxylating intermediate produced from quinone photolysis in question.

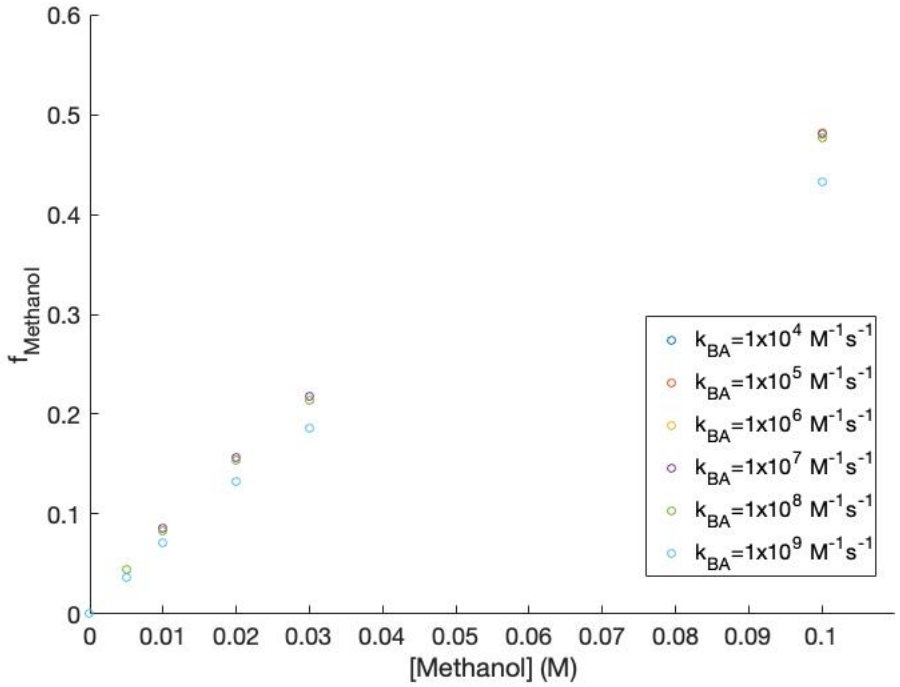

Figure 13. Fraction of triplet quinone reacting with methanol, as described by eq 10, in an aqueous aerobic system containing benzoic acid and varying concentrations of methanol. Concentrations of methanol used in quenching experiments ranged between 0.005 – 0.1 M.

ENVIRONMENTAL IMPLICATIONS

The results presented in this study have several implications for measurement of hydroxylating species formation from DOM photolysis. Testing both benzoic acid and benzene as probe compound shed light on their respective effectiveness as probe compound for hydroxyl radials and, more generally, hydroxylating species. Additionally, the quenching of phenol formation from benzene during quinone photolysis by methanol indicates that methanol reacts with both •OH and •OH -like species. Although this result has been demonstrated in the literature, methanol has not been used explicitly to assess the reactivity of •OH-like species derived from triplet quinones.

A recent study by Leresche et al. measuring the hydroxylating capacity of DOM before and after ozonation attributed the increase in quantum yields for hydroxylating species to the increase in quinone content of DOM post-oxidation.[47] The results presented here support the hypothesis that ^{3}DOM*, including quinones, are precursors of •OH and •OH-like species from DOM photolysis. However, another recent study suggested that ^{3}DOM* is not a major precursor to •OH or •OH-like species based on correlations between RI quantum yields and the abundance of various formulas from ultra-high-resolution mass spectrometry.[66] Instead, it was suggested that ^{1}DOM*, charge-transfer states, or exciplexes involving photochemically excited DOM may be involved.[66] This hypothesis is consistent with the role of hydroxybenzoic acids as Sens, but not with quinones. This thesis contends that triplet quinones are likely responsible for some of the hydroxylation reactions observed for aromatic probe compounds given the known presence of these moieties in DOM. Additionally, these results demonstrate that quinones do not necessarily need to be photostable to contribute significantly to the •OH or •OH-like production. For example, similar rates of hydroxylation reactions were observed for hydroquinone, a phenol photoproduct.

To assess the role of Sens for production of •OH and •OH-like species, the contribution of quinones and hydroxybenzoic acids to the fraction of light absorbed by DOM was calculated, using electrochemical data for Suwannee River fulvic acid (SRFA).[67] Similar calculations were done in a study by Ma et al. (2010).[68] It should be noted that electron donating capacity (EDC) and the electron accepting capacity (EAC) measurements are dependent on solutions conditions, which might not be identical to solution conditions of DOM photochemistry experiments. Electron accepting capacities (EAC, $\mu mol_{e-}\ g_{HS}^{-1}$) were used to calculate the concentration of quinones (EAC $\times\ \mu mol_{quinone}/2\ \mu mol_{e-}$) and electron donating capacities (EDC, $\mu mol_{e-}\ g_{HS}^{-1}$) were used to calculate the concentration of hydroxybenzoic acids (EDC $\times\ \mu mol_{hydroxybenzoic\ acid}/2\ \mu mol_{e-}$). By assuming that the EDC is due to hydroxybenzoic acids, the calculations shown here represent an upper limit for the contribution of hydroxybenzoic acids to DOM absorbance, with the actual contribution likely being less. EDC and EAC measurements are dependent on solutions conditions, which might not be identical to solution conditions of DOM photochemistry experiments. The absorbance due to quinones and hydroxybenzoic acids was calculated by multiplying the above calculated concentrations by the molar absorption coefficient for these compounds measured in our study. The results of these calculations are shown in Figure 14 and in Table 5. For calculations, SRFA was used as a model DOM sample. The concentration of quinones in SRFA was calculated using the EAC value of 671 $\mu mol_{e-}\ g_{HS}^{-1}$ measured by Aeschbacher et al. (2010), [67] with the quinone content being 335.5 $\mu mol_{quinone}\ g_{HS}^{-1}$. Finally, the absorbance at a specific wavelength was calculated by selecting a quinone Sens (e.g., *p*-benzoquinone), assuming the entire [quinone] calculated above is attributable to that specific quinone and multiplying by the molar extinction coefficient. For example, for p-benzoquinone at 246 nm: $Abs_{pBQ,246} = 3.35\ \mu mol_{pBQ}\ L^{-1} \times 22{,}000\ M^{-1}\ cm^{-1} = 0.074\ cm^{-1}$. To determine the fraction of light absorbed by a given quinone in the SRFA mixture the DOM solution

absorbance was calculated using a measured $SUVA_{254}$ (4.2 L mg_C^{-1} m^{-1}) and spectral slope (*S*, 0.0152 nm^{-1}) for SRFA: $Abs_{SRFA,246} = SUVA_{254} \times \exp(-S(246\text{-}250)) \times 0.01$ cm $m^{-1} \times 5$ mg_C L^{-1} = 0.24 cm^{-1}. The fraction of light absorbed by *p*-benzoquinone at 246 nm is therefore equal to 0.074/0.24 = 0.31. For the hydroxybenzoic acid Sens, 4HBA and DHBA, the fraction of light absorbed at 300 nm ranged from 0.2% by 4HBA to 47.9% by DHBA, whereas at 254 nm the fraction of light absorbed by 4HBA is 86.0% and the fraction of light absorbed by DHBA is 47.9% (Table 5). Figure 14A shows that the fraction of light absorbed by quinones depends on the specific compound and wavelength. As a surrogate for the variety of quinone structures in a given DOM sample eight quinones were used to approximate the total quinone absorbance, shown in Figure 14B. In this approximation (Figure 14B) quinone absorbance falls in the 1.5 – 22% range. For two quinone Sens in this study (PBQ and DPBQ), values ranged between nearly 31% (by PBQ at 246 nm) and <1% (by PBQ at 424 nm). For quinones whose absorption spectrum extends into the far UV and visible, the fraction of light absorbed at longer wavelengths increases (e.g., 15.2 % by 1,4-napthoquinone at 342 nm). For DPBQ, the product of the observed quantum yield at 254 nm as an estimate for the quinone quantum yield (17×10^{-3}, Table 4) and the fraction of light absorbed by the mixture of quinones at within the range of wavelengths shown in Figure 14B (1.5 – 22%), at 254 nm the quantum yield would be ~ 4.8×10^{-3}. A study by Lester et al. showed that quantum yields for the formation of hydroxylating species from DOM photolysis at 254 nm is generally an order of magnitude higher than the quantum yield values at wavelengths greater than 300 nm, with the quantum yield for the formation of hydroxylating species from SRFA being 0.047.[69]

Table 5. Fractional absorbance of quinone and hydroxybenzoic acid Sens in SRFA (2S101F) calculated based on electron accepting capacity and electron donating capacity, respectively.

Quinone	Wavelength (nm)	Epsilon (M^{-1} cm^{-1})	Abs SRFA (cm^{-1})	Abs MS (cm^{-1})	Abs MS/Abs SRFA × 100
p-benzoquinone	246	22000	0.24	0.074	31.1%
	296	320	0.11	0.001	1.0%
	424	20	0.02	0.000	0.4%
2,6-dimethoxy-p-benzoquinone	258	17000	0.20	0.057	28.9%
	332	280	0.06	0.001	1.5%
	424	30	0.02	0.000	0.6%
1,4-napthoquinone	252	16700	0.22	0.056	25.9%
	342	2490	0.06	0.008	15.2%
4-hydroxybenzoic acid	254	12676	0.21	0.181	86.0%
	300	11	0.10	0.000	0.2%
2,4-dihydroxybenzoic acid	254	9296	0.21	0.132	63.0%
	300	3510	0.10	0.050	47.9%

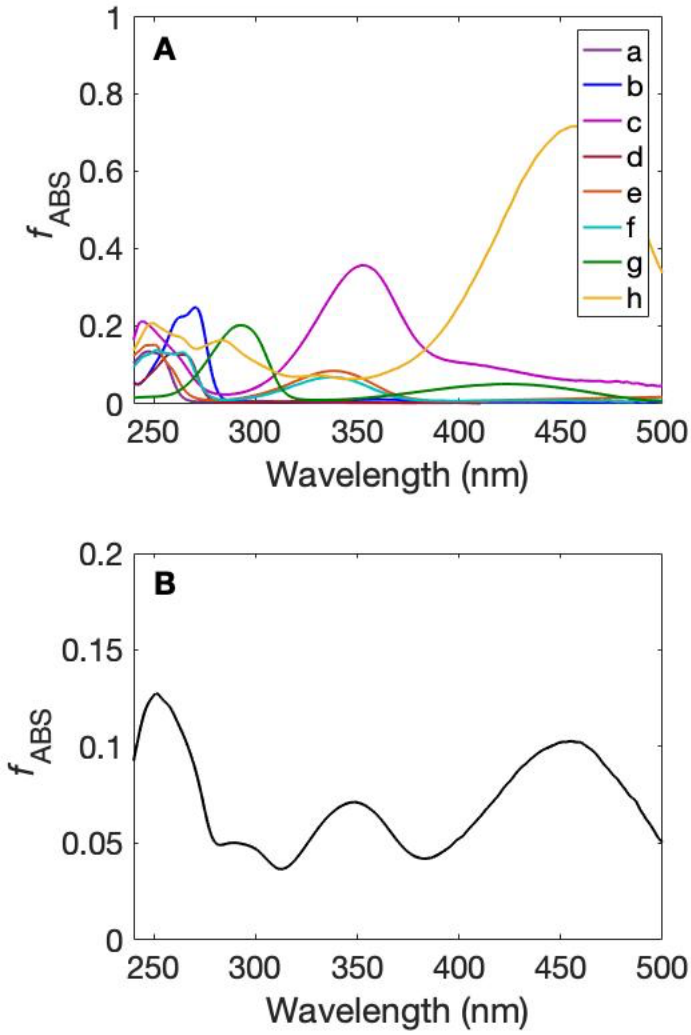

Figure 14. Fraction of light absorbed (f_{ABS}) by quinones in DOM. **A:** Fraction of light absorbance by a: p-benzoquinone, b: 2,3,5,6-tetramethyl-1,4-benzoquinone, c: 2,5-diphenyl-1,4-benzoquinone, d: 2,5-di-tert-butyl-1,4-benzoquinone, e: 1,4-naphthoquinone, f: 2-methyl-1,4-naphthoquinone, g: 2,6-dimethoxy-p-benzoquinone, and h: alizarin, calculated individually, as though each account for entirety of quinone content in SRFA. **B:** Fraction of absorbance by quinones a – h from above to account for quinone content of DOM in equal parts (12.5% each).

Taken as a whole, the results of this study provide further support for the role of quinones and hydroxybenzoic acids as Sens for the production hydroxylating species from DOM photolysis. An important finding is that photoproducts from these species, especially in the case of quinones, likely have a hydroxylating capacity as well. Methanol quenching as a test of hydroxylating species' identity was inclusive, indicating that other quenchers are needed to assess these differences

in reactivity. Additionally, the quantum yields of •OH and •OH-like species from Sens photolysis are comparable to values measured for DOM by taking into account the fraction of light absorbed by quinones within DOM. These results indicate that triplet state quinones play a role in the hydroxylating capacity of DOM.

ACKNOWLEDGEMENTS

Funding for this study came from the US National Science Foundation (CBET #1453906 and CHE #1808126) and through the University of Colorado Discovery Learning Apprenticeship.

REFERENCES

(1) Southworth, B. A.; Voelker, B. M. Hydroxyl Radical Production via the Photo-Fenton Reaction in the Presence of Fulvic Acid. *Environ. Sci. Technol.* **2003**, *37* (6), 1130–1136. https://doi.org/10.1021/es020757l.

(2) Vaughan, P. P.; Blough, N. V. Photochemical Formation of Hydroxyl Radical by Constituents of Natural Waters. *Environ. Sci. Technol.* **1998**, *32* (19), 2947–2953. https://doi.org/10.1021/es9710417.

(3) Vione, D.; Falletti, G.; Maurino, V.; Minero, C.; Pelizzetti, E.; Malandrino, M.; Ajassa, R.; Olariu, R.-I.; Arsene, C. Sources and Sinks of Hydroxyl Radicals upon Irradiation of Natural Water Samples. *Environ. Sci. Technol.* **2006**, *40* (12), 3775–3781. https://doi.org/10.1021/es052206b.

(4) Wenk, J.; von Gunten, U.; Canonica, S. Effect of Dissolved Organic Matter on the Transformation of Contaminants Induced by Excited Triplet States and the Hydroxyl Radical. *Environ. Sci. Technol.* **2011**, *45* (4), 1334–1340. https://doi.org/10.1021/es102212t.

(5) Xu, H.; Cooper, W. J.; Jung, J.; Song, W. Photosensitized Degradation of Amoxicillin in Natural Organic Matter Isolate Solutions. *Water Research* **2011**, *45* (2), 632–638. https://doi.org/10.1016/j.watres.2010.08.024.

(6) Boreen, A. L.; Arnold, W. A.; McNeill, K. Photodegradation of Pharmaceuticals in the Aquatic Environment: A Review. *Aquatic Sciences - Research Across Boundaries* **2003**, *65* (4), 320–341. https://doi.org/10.1007/s00027-003-0672-7.

(7) Buxton, G. V.; Greenstock, C. L.; Helman, W. P.; Ross, A. B. Critical Review of Rate Constants for Reactions of Hydrated Electrons, Hydrogen Atoms and Hydroxyl Radicals (·OH/·O−) in Aqueous Solution. *Journal of Physical and Chemical Reference Data* **1988**, *17* (2), 513–886. https://doi.org/10.1063/1.555805.

(8) Latch, D. E.; Stender, B. L.; Packer, J. L.; Arnold, W. A.; McNeill, K. Photochemical Fate of Pharmaceuticals in the Environment: Cimetidine and Ranitidine. *Environ. Sci. Technol.* **2003**, *37* (15), 3342–3350. https://doi.org/10.1021/es0340782.

(9) McConville, M. B.; Mezyk, S. P.; Remucal, C. K. Indirect Photodegradation of the Lampricides TFM and Niclosamide. *Environ. Sci.: Processes Impacts* **2017**, *19* (8), 1028–1039. https://doi.org/10.1039/C7EM00208D.

(10) McNeill, K.; Canonica, S. Triplet State Dissolved Organic Matter in Aquatic Photochemistry: Reaction Mechanisms, Substrate Scope, and Photophysical Properties. *Environ. Sci.: Processes Impacts* **2016**, *18* (11), 1381–1399. https://doi.org/10.1039/C6EM00408C.

(11) Packer, J. L.; Werner, J. J.; Latch, D. E.; McNeill, K.; Arnold, W. A. Photochemical Fate of Pharmaceuticals in the Environment: Naproxen, Diclofenac, Clofibric Acid, and Ibuprofen. *Aquatic Sciences - Research Across Boundaries* **2003**, *65* (4), 342–351. https://doi.org/10.1007/s00027-003-0671-8.

(12) Scully, F. E.; Hoigné, J. Rate Constants for Reactions of Singlet Oxygen with Phenols and Other Compounds in Water. *Chemosphere* **1987**, *16* (4), 681–694. https://doi.org/10.1016/0045-6535(87)90004-X.

(13) Rosario-Ortiz, F. L.; Canonica, S. Probe Compounds to Assess the Photochemical Activity of Dissolved Organic Matter. *Environ. Sci. Technol.* **2016**, *50* (23), 12532–12547. https://doi.org/10.1021/acs.est.6b02776.

(14) Vione, D.; Minella, M.; Maurino, V.; Minero, C. Indirect Photochemistry in Sunlit Surface Waters: Photoinduced Production of Reactive Transient Species. *Chem. Eur. J.* **2014**, *20* (34), 10590–10606. https://doi.org/10.1002/chem.201400413.
(15) Miller, C. J.; Rose, A. L.; Waite, T. D. Hydroxyl Radical Production by H2O2-Mediated Oxidation of Fe(II) Complexed by Suwannee River Fulvic Acid Under Circumneutral Freshwater Conditions. *Environ. Sci. Technol.* **2013**, *47* (2), 829–835. https://doi.org/10.1021/es303876h.
(16) White, E. M.; Vaughan, P. P.; Zepp, R. G. Role of the Photo-Fenton Reaction in the Production of Hydroxyl Radicals and Photobleaching of Colored Dissolved Organic Matter in a Coastal River of the Southeastern United States. *Aquatic Sciences - Research Across Boundaries* **2003**, *65* (4), 402–414. https://doi.org/10.1007/s00027-003-0675-4.
(17) Mopper, K.; Zhou, X. Hydroxyl Radical Photoproduction in the Sea and Its Potential Impact on Marine Processes. *Science* **1990**, *250* (4981), 661–664. https://doi.org/10.1126/science.250.4981.661.
(18) Page, S. E.; Arnold, W. A.; McNeill, K. Assessing the Contribution of Free Hydroxyl Radical in Organic Matter-Sensitized Photohydroxylation Reactions. *Environ. Sci. Technol.* **2011**, *45* (7), 2818–2825. https://doi.org/10.1021/es2000694.
(19) Gan, D.; Jia, M.; Vaughan, P. P.; Falvey, D. E.; Blough, N. V. Aqueous Photochemistry of Methyl-Benzoquinone. *J. Phys. Chem. A* **2008**, *112* (13), 2803–2812. https://doi.org/10.1021/jp710724e.
(20) McKay, G.; Rosario-Ortiz, F. L. Temperature Dependence of the Photochemical Formation of Hydroxyl Radical from Dissolved Organic Matter. *Environ. Sci. Technol.* **2015**, *49* (7), 4147–4154. https://doi.org/10.1021/acs.est.5b00102.
(21) Pochon, A.; Vaughan, P. P.; Gan, D.; Vath, P.; Blough, N. V.; Falvey, D. E. Photochemical Oxidation of Water by 2-Methyl-1,4-Benzoquinone: Evidence against the Formation of Free Hydroxyl Radical. *J. Phys. Chem. A* **2002**, *106* (12), 2889–2894. https://doi.org/10.1021/jp012856b.
(22) Sun, L.; Qian, J.; Blough, N. V.; Mopper, K. Insights into the Photoproduction Sites of Hydroxyl Radicals by Dissolved Organic Matter in Natural Waters. *Environ. Sci. Technol. Lett.* **2015**, *2* (12), 352–356. https://doi.org/10.1021/acs.estlett.5b00294.
(23) Vione, D.; Ponzo, M.; Bagnus, D.; Maurino, V.; Minero, C.; Carlotti, M. E. Comparison of Different Probe Molecules for the Quantification of Hydroxyl Radicals in Aqueous Solution. *Environ Chem Lett* **2010**, *8* (1), 95–100. https://doi.org/10.1007/s10311-008-0197-3.
(24) Zepp, R. G.; Baughman, G. L.; Schlotzhauer, P. F. Comparison of Photochemical Behavior of Various Humic Substances in Water: II. Photosensitized Oxygenations. *Chemosphere* **1981**, *10* (1), 119–126. https://doi.org/10.1016/0045-6535(81)90175-2.
(25) Canonica, Silvio.; Jans, Urs.; Stemmler, Konrad.; Hoigne, Jurg. Transformation Kinetics of Phenols in Water: Photosensitization by Dissolved Natural Organic Material and Aromatic Ketones. *Environ. Sci. Technol.* **1995**, *29* (7), 1822–1831. https://doi.org/10.1021/es00007a020.
(26) Vialykh, E. A.; McKay, G.; Rosario-Ortiz, F. L. Computational Assessment of the Three-Dimensional Configuration of Dissolved Organic Matter Chromophores and Influence on Absorption Spectra. *Environ. Sci. Technol.* **2020**, *54* (24), 15904–15913. https://doi.org/10.1021/acs.est.0c05860.

(27) McKay, G.; Korak, J. A.; Erickson, P. R.; Latch, D. E.; McNeill, K.; Rosario-Ortiz, F. L. The Case Against Charge Transfer Interactions in Dissolved Organic Matter Photophysics. *Environ. Sci. Technol.* **2018**, *52* (2), 406–414. https://doi.org/10.1021/acs.est.7b03589.
(28) Del Vecchio, R.; Blough, N. V. On the Origin of the Optical Properties of Humic Substances. *Environ. Sci. Technol.* **2004**, *38* (14), 3885–3891. https://doi.org/10.1021/es049912h.
(29) Sharpless, C. M.; Blough, N. V. The Importance of Charge-Transfer Interactions in Determining Chromophoric Dissolved Organic Matter (CDOM) Optical and Photochemical Properties. *Environ. Sci.: Processes Impacts* **2014**, *16* (4), 654–671. https://doi.org/10.1039/C3EM00573A.
(30) Burns, J. M.; Cooper, W. J.; Ferry, J. L.; King, D. W.; DiMento, B. P.; McNeill, K.; Miller, C. J.; Miller, W. L.; Peake, B. M.; Rusak, S. A.; Rose, A. L.; Waite, T. D. Methods for Reactive Oxygen Species (ROS) Detection in Aqueous Environments. *Aquat Sci* **2012**, *74* (4), 683–734. https://doi.org/10.1007/s00027-012-0251-x.
(31) Dong, M. M.; Rosario-Ortiz, F. L. Photochemical Formation of Hydroxyl Radical from Effluent Organic Matter. *Environ. Sci. Technol.* **2012**, *46* (7), 3788–3794. https://doi.org/10.1021/es2043454.
(32) Ononye, A. I.; McIntosh, A. R.; Bolton, J. R. Mechanism of the Photochemistry of P-Benzoquinone in Aqueous Solutions. 1. Spin Trapping and Flash Photolysis Electron Paramagnetic Resonance Studies. *J. Phys. Chem.* **1986**, *90* (23), 6266–6270. https://doi.org/10.1021/j100281a039.
(33) Page, S. E.; Arnold, W. A.; McNeill, K. Terephthalate as a Probe for Photochemically Generated Hydroxyl Radical. *J. Environ. Monit.* **2010**, *12* (9), 1658. https://doi.org/10.1039/c0em00160k.
(34) Alegria, A. E.; Ferrer, A.; Sepulveda, E. Photochemistry of Water-Soluble Quinones. Production of a Water-Derived Spin Adduct. *Photochem Photobiol* **1997**, *66* (4), 436–442. https://doi.org/10.1111/j.1751-1097.1997.tb03170.x.
(35) Alegría, A. E.; Ferrer, A.; Santiago, G.; Sepúlveda, E.; Flores, W. Photochemistry of Water-Soluble Quinones. Production of the Hydroxyl Radical, Singlet Oxygen and the Superoxide Ion. *Journal of Photochemistry and Photobiology A: Chemistry* **1999**, *127* (1–3), 57–65. https://doi.org/10.1016/S1010-6030(99)00138-0.
(36) Ononye, A. I.; Bolton, J. R. Mechanism of the Photochemistry of P-Benzoquinone in Aqueous Solutions. 2. Optical Flash Photolysis Studies. *J. Phys. Chem.* **1986**, *90* (23), 6270–6274. https://doi.org/10.1021/j100281a040.
(37) von Sonntag, J.; Mvula, E.; Hildenbrand, K.; von Sonntag, C. Photohydroxylation of 1,4-Benzoquinone in Aqueous Solution Revisited. *Chem. Eur. J.* **2004**, *10* (2), 440–451. https://doi.org/10.1002/chem.200305136.
(38) Pou, S.; Hassett, D. J.; Britigan, B. E.; Cohen, M. S.; Rosen, G. M. Problems Associated with Spin Trapping Oxygen-Centered Free Radicals in Biological Systems. *Analytical Biochemistry* **1989**, *177* (1), 1–6. https://doi.org/10.1016/0003-2697(89)90002-X.
(39) Eberson, L.; Persson, O. Generation of Acyloxyl Spin Adducts from N-Tert-Butyl- -Phenyl-Nitrone † (PBN) and 4,5-Dihydro-5,5-Dimethylpyrrole 1-Oxide (DMPO) via Nonconventional Mechanisms. *Journal of the Chemical Society, Perkin Transactions 2* **1997**, 1689–1696.

(40) Görner, H. Photoreactions of P-Quinones with Dimethyl Sulfide and Dimethyl Sulfoxide in Aqueous Acetonitrile†. *Photochemistry and Photobiology* **2006**, *82* (1), 71–77. https://doi.org/10.1562/2005-05-25-RA-540.
(41) Beck, S. M.; Brus, L. E. Photooxidation of Water by P-Benzoquinone. *J. Am. Chem. Soc.* **1982**, *104* (4), 1103–1104. https://doi.org/10.1021/ja00368a036.
(42) Görner, H. Photoprocesses of P-Benzoquinones in Aqueous Solution. *J. Phys. Chem. A* **2003**, *107* (51), 11587–11595. https://doi.org/10.1021/jp030789a.
(43) Loeff, I.; Treinin, A.; Linschitz, H. Photochemistry of 9,10-Anthraquinone-2-Sulfonate in Solution. 1. Intermediates and Mechanism. *J. Phys. Chem.* **1983**, *87* (14), 2536–2544. https://doi.org/10.1021/j100237a017.
(44) Taniguchi, M.; Lindsey, J. S. Database of Absorption and Fluorescence Spectra of >300 Common Compounds for Use in PhotochemCAD. *Photochemistry and Photobiology* **2018**, *94* (2), 290–327. https://doi.org/10.1111/php.12860.
(45) Jin, S.; Mofidi, A. A.; Linden, K. G. Polychromatic UV Fluence Measurement Using Chemical Actinometry, Biodosimetry, and Mathematical Techniques. *J. Environ. Eng.* **2006**, *132* (8), 831–841. https://doi.org/10.1061/(ASCE)0733-9372(2006)132:8(831).
(46) Laszakovits, J. R.; Berg, S. M.; Anderson, B. G.; O'Brien, J. E.; Wammer, K. H.; Sharpless, C. M. P-Nitroanisole/Pyridine and p-Nitroacetophenone/Pyridine Actinometers Revisited: Quantum Yield in Comparison to Ferrioxalate. *Environ. Sci. Technol. Lett.* **2017**, *4* (1), 11–14. https://doi.org/10.1021/acs.estlett.6b00422.
(47) Leresche, F.; Torres-Ruiz, J. A.; Kurtz, T.; von Gunten, U.; Rosario-Ortiz, F. L. Optical Properties and Photochemical Production of Hydroxyl Radical and Singlet Oxygen after Ozonation of Dissolved Organic Matter. *Environ. Sci.: Water Res. Technol.* **2021**, *7* (2), 346–356. https://doi.org/10.1039/D0EW00878H.
(48) Garg, S.; Rose, A. L.; Waite, T. D. Photochemical Production of Superoxide and Hydrogen Peroxide from Natural Organic Matter. *Geochimica et Cosmochimica Acta* **2011**, *75* (15), 4310–4320. https://doi.org/10.1016/j.gca.2011.05.014.
(49) Garg, S.; Rose, A. L.; Waite, T. D. Production of Reactive Oxygen Species on Photolysis of Dilute Aqueous Quinone Solutions. *Photochemistry and Photobiology* **2007**, *83* (4), 904–913. https://doi.org/10.1111/j.1751-1097.2007.00075.x.
(50) Goldstein, S.; Aschengrau, D.; Diamant, Y.; Rabani, J. Photolysis of Aqueous H2O2: Quantum Yield and Applications for Polychromatic UV Actinometry in Photoreactors. *Environ. Sci. Technol.* **2007**, *41* (21), 7486–7490. https://doi.org/10.1021/es071379t.
(51) Rabani, J.; Klug-Roth, D.; Henglein, A. Pulse Radiolytic Investigations of OHCH2O2 Radicals. *J. Phys. Chem.* **1974**, *78* (21), 2089–2093. https://doi.org/10.1021/j100614a005.
(52) Chu, L.; Anastasio, C. Temperature and Wavelength Dependence of Nitrite Photolysis in Frozen and Aqueous Solutions. *Environ. Sci. Technol.* **2007**, *41* (10), 3626–3632. https://doi.org/10.1021/es062731q.
(53) Arakaki, T.; Faust, B. C. Sources, Sinks, and Mechanisms of Hydroxyl Radical (•OH) Photoproduction and Consumption in Authentic Acidic Continental Cloud Waters from Whiteface Mountain, New York: The Role of the Fe(r) (r = II, III) Photochemical Cycle. *Journal of Geophysical Research: Atmospheres* **1998**, *103* (D3), 3487–3504. https://doi.org/10.1029/97JD02795.
(54) Balakrishnan, I.; Reddy, M. P. Effect of Temperature on the Gamma Radiolysis of Aqueous Solutions. *J. Phys. Chem.* **1972**, *76* (9), 1273–1279. https://doi.org/10.1021/j100653a008.

(55) Charbouillot, T.; Brigante, M.; Mailhot, G.; Maddigapu, P. R.; Minero, C.; Vione, D. Performance and Selectivity of the Terephthalic Acid Probe for OH as a Function of Temperature, PH and Composition of Atmospherically Relevant Aqueous Media. *Journal of Photochemistry and Photobiology A: Chemistry* **2011**, *222* (1), 70–76. https://doi.org/10.1016/j.jphotochem.2011.05.003.

(56) Deister, U.; Warneck, P.; Wurzinger, C. OH Radicals Generated by NO3- Photolysis in Aqueous Solution: Competition Kinetics and a Study of the Reaction OH + CH2(OH)SO3- . *Berichte der Bunsengesellschaft für physikalische Chemie* **1990**, *94*, 594–599.

(57) Van Buren, J.; Prasse, C.; Marron, E. L.; Skeel, B.; Sedlak, D. L. Ring-Cleavage Products Produced during the Initial Phase of Oxidative Treatment of Alkyl-Substituted Aromatic Compounds. *Environ. Sci. Technol.* **2020**, *54* (13), 8352–8361. https://doi.org/10.1021/acs.est.0c00432.

(58) Sun, L.; Chen, H.; Abdulla, H. A.; Mopper, K. Estimating Hydroxyl Radical Photochemical Formation Rates in Natural Waters during Long-Term Laboratory Irradiation Experiments. *Environ. Sci.: Processes Impacts* **2014**, *16* (4), 757–763. https://doi.org/10.1039/C3EM00587A.

(59) Qian, J.; Mopper, K.; Kieber, D. J. Photochemical Production of the Hydroxyl Radical in Antarctic Waters. *Deep Sea Research Part I: Oceanographic Research Papers* **2001**, *48* (3), 741–759. https://doi.org/10.1016/S0967-0637(00)00068-6.

(60) Görner, H. Photoreduction of 9,10-Anthraquinone Derivatives: Transient Spectroscopy and Effects of Alcohols and Amines on Reactivity in Solution¶. *Photochemistry and Photobiology* **2003**, *77* (2), 171–179. https://doi.org/10.1562/0031-8655(2003)0770171POADTS2.0.CO2.

(61) Görner, H. Photoreduction of P-Benzoquinones: Effects of Alcohols and Amines on the Intermediates and Reactivities in Solution¶. *Photochemistry and Photobiology* **2003**, *78* (5), 440–448. https://doi.org/10.1562/0031-8655(2003)0780440POPEOA2.0.CO2.

(62) Görner, H. Photoinduced Oxygen Uptake for 9,10-Anthraquinone in Air-Saturated Aqueous Acetonitrile in the Presence of Formate, Alcohols, Ascorbic Acid or Amines. *Photochem. Photobiol. Sci.* **2006**, *5* (11), 1052–1058. https://doi.org/10.1039/B606968A.

(63) Jonsson, M.; Lind, J.; Reitberger, T.; Eriksen, T. E.; Merenyi, G. Redox Chemistry of Substituted Benzenes: The One-Electron Reduction Potentials of Methoxy-Substituted Benzene Radical Cations. *J. Phys. Chem.* **1993**, *97* (43), 11278–11282. https://doi.org/10.1021/j100145a027.

(64) Zellner, R.; Exner, M.; Herrmann, H. Absolute OH Quantum Yields in the Laser Photolysis of Nitrate, Nitrite and Dissolved H202 at 308 and 351 Nm in the Temperature Range 278-353 K. *Journal of Atmospheric Chemistry* **1990**, *10*, 411–425.

(65) Sur, B.; Rolle, M.; Minero, C.; Maurino, V.; Vione, D.; Brigante, M.; Mailhot, G. Formation of Hydroxyl Radicals by Irradiated 1-Nitronaphthalene (1NN): Oxidation of Hydroxyl Ions and Water by the 1NN Triplet State. *Photochemical & Photobiological Sciences* **2011**, *10* (11), 1817–1824. https://doi.org/10.1039/C1PP05216K.

(66) Berg, S. M.; Whiting, Q. T.; Herrli, J. A.; Winkels, R.; Wammer, K. H.; Remucal, C. K. The Role of Dissolved Organic Matter Composition in Determining Photochemical Reactivity at the Molecular Level. *Environ. Sci. Technol.* **2019**, *53* (20), 11725–11734. https://doi.org/10.1021/acs.est.9b03007.

(67) Aeschbacher, M.; Sander, M.; Schwarzenbach, R. P. Novel Electrochemical Approach to Assess the Redox Properties of Humic Substances. *Environ. Sci. Technol.* **2010**, *44* (1), 87–93. https://doi.org/10.1021/es902627p.
(68) Ma, J.; Del Vecchio, R.; Golanoski, K. S.; Boyle, E. S.; Blough, N. V. Optical Properties of Humic Substances and CDOM: Effects of Borohydride Reduction. *Environ. Sci. Technol.* **2010**, *44* (14), 5395–5402. https://doi.org/10.1021/es100880q.
(69) Lester, Y.; Sharpless, C. M.; Mamane, H.; Linden, K. G. Production of Photo-Oxidants by Dissolved Organic Matter During UV Water Treatment. *Environ. Sci. Technol.* **2013**, *47* (20), 11726–11733. https://doi.org/10.1021/es402879x.